



**Mechanism, Thermochemistry, and Kinetics of the  
Reversible Reactions:  $C_2H_3 + H_2 \rightleftharpoons C_2H_4 + H \rightleftharpoons C_2H_5$**

Journal:	<i>Faraday Discussions</i>
Manuscript ID	FD-ART-12-2021-000124.R1
Article Type:	Paper
Date Submitted by the Author:	25-Feb-2022
Complete List of Authors:	Nguyen, Thanh Lam; University of Florida, Physics and Chemistry Bross, David; Argonne National Laboratory, Chemical Science and Engineering Division Ruscic, Branko; Argonne National Laboratory, Chemical Sciences and Engineering Division; University of Chicago, Computation Institute Ellison, G.; UCB 215, Department of Chemistry and Biochemistry Stanton, John ; u florida,

## Mechanism, Thermochemistry, and Kinetics of the Reversible Reactions:



Thanh Lam Nguyen,<sup>1</sup> David H. Bross,<sup>2</sup> Branko Ruscic,<sup>2</sup> G. Barney Ellison,<sup>3</sup> and John F. Stanton\*,<sup>1</sup>

<sup>1</sup>Quantum Theory Project, Departments of Chemistry and Physics, University of Florida, Gainesville, FL 32611 (USA).

<sup>2</sup>Chemical Sciences and Engineering Division, Argonne National Laboratory, Lemont, Illinois 60439, United States.

<sup>3</sup>Department of Chemistry, University of Colorado, Boulder, CO 80309 (USA).

Corresponding author: [johnstanton@ufl.edu](mailto:johnstanton@ufl.edu)

High-level coupled cluster theory, in conjunction with Active Thermochemical Tables (ATcT) and E,J-resolved master equation calculations were used in a study of the title reactions, which play an important role in combustion of hydrocarbons. In the set of radical/radical reactions leading to soot formation in flames, addition of H-atoms to alkenes is likely a common reaction triggering the isomerization of complex hydrocarbons to aromatics. Heats of formation of C<sub>2</sub>H<sub>3</sub>, C<sub>2</sub>H<sub>4</sub>, and C<sub>2</sub>H<sub>5</sub> are established to be 301.26 ± 0.30 at 0 K (297.22 ± 0.30 at 298 K), 60.89 ± 0.11 (52.38 ± 0.11), and 131.38 ± 0.22 (120.63 ± 0.22) kJ mol<sup>-1</sup>, respectively. The calculated rate constants from first principles agree well with experiments where they are available. Under conditions typical of high temperature combustion – where experimental work is very challenging with a consequent dearth of accurate data – we provide high-level theoretical results for kinetic modeling.

## INTRODUCTION

Vinyl ( $C_2H_3$ ), ethene ( $C_2H_4$ ), and ethyl ( $C_2H_5$ ) are key intermediates in flames of methane, acetylene, and hydrocarbons in general.<sup>1, 2</sup> High accuracy thermochemical parameters, kinetics and mechanisms of their reactions with other species facilitate better understanding of combustion chemistry as well as help optimize the combustion process.<sup>3</sup> As detailed later in this work, rate constants for the title reactions are rather rare despite their importance. Surprisingly, most available experimental results arise from indirect measurements,<sup>4-10</sup> and are thus highly uncertain.<sup>2, 5</sup> In this work, we study the reversible reactions below (Eqs. 1-2) using parameters from a high accuracy thermochemistry method (ATcT)<sup>11, 12, 13</sup> and quantum chemical calculations in combination with two-dimensional master equation techniques (2DME)<sup>14-18</sup> to obtain phenomenological rate constants as functions of both temperature and pressure.



The kinetics analyses are based on a very accurate potential energy surface (PES) constructed with high-level quantum chemistry (HEAT).<sup>19-21</sup>

### Active Thermochemical Tables Approach

The Active Thermochemical Tables (ATcT) approach – a paradigm for obtaining reliable and accurate thermochemical quantities – has been described in considerable detail elsewhere.<sup>11, 12</sup> Tersely, instead of using conventional sequential thermochemistry (A begets B, B begets C, etc.), ATcT are based on constructing, statistically analyzing, and solving a thermochemical network (TN) simultaneously for all included chemical species. Rather than incorporating enthalpies of

formation *per se*, the TN is constructed from actual thermochemical determinations, such as bond dissociation energies, reaction enthalpies, equilibrium constants, ionization energies, electron affinities, etc. All available high-quality thermochemical determinations are included, regardless of whether they originated from experiments (actual measurements) or theoretical treatments (virtual measurements). These determinations effectively provide the pertinent interdependences between the thermochemistry of the involved chemical species, and, together with their associated uncertainties, constitute a set of conditional constraints that must be fulfilled by the resulting enthalpies of formation. However, since determinations have finite accuracies, the TN constraints are not necessarily entirely mutually consistent. Potential inconsistencies between various determinations are explored by ATcT via an iterative statistical analysis, the focus of which is the identification of determinations with 'optimistic' uncertainties that are likely to unduly skew the final results. Once the TN is self-consistent, ATcT solves it and produces the final enthalpies of formation simultaneously for all included chemical species.

The results presented here are based on the ATcT TN ver. 1.124, which incorporates >2,750 species, interconnected by >29,000 experimental and theoretical determinations, and was very recently utilized to report the most up-to-date thermochemistry of  $\text{CH}_n$ ,  $n = 4 - 0$  species together with nonrigid rotor anharmonic oscillator (NRRAO) corrected thermophysical properties of methyl and methylene.<sup>22</sup> In addition, the same version of ATcT results was used to carry out the benchmarking of a state-of-the-art composite electronic structure approach that aims to reproduce total atomization energies of small molecules within  $10\text{-}15\text{ cm}^{-1}$ .<sup>23</sup> ATcT TN ver. 1.124 is a successor to ver. 1.122x that was used in a recent study of C–H bond dissociation enthalpies

(BDE) of aromatic aldehydes,<sup>24</sup> itself being a result of successive expansions of earlier versions, such as 1.122h,<sup>25</sup> 1.122o,<sup>26</sup> 1.122p,<sup>27</sup> 1.122q,<sup>28, 29</sup> 1.122r,<sup>30</sup> and 1.122v.<sup>31</sup>

## High Accuracy Coupled-Cluster Calculations

All relevant stationary points on the PES of  $C_2H_5$  for reactions (1) and (2) were computed using a slight modification of the HEAT-345Q protocol.<sup>19-21</sup> More details about the methodology can be found elsewhere;<sup>19-21</sup> a brief summary is given here. HEAT is a composite method which uses the ae-CCSD(T)/cc-pVQZ level of theory to obtain optimized geometries, followed by single-point energy calculations. In HEAT-345Q, the SCF energies are extrapolated to the complete basis set limit (CBS) using Dunning's aug-cc-pCVXZ basis sets<sup>32</sup> (where X = T, Q, and 5) and the CCSD(T) electron correlation energies are extrapolated using X = Q and 5. Higher level corrections for electron correlation are also included using iterative triple- (CCSDT) and quadruple-excitation (CCSDTQ) methods.<sup>33</sup> Anharmonic vibrational zero-point energies (ZPE) are computed using second-order vibrational perturbation theory (VPT2)<sup>34</sup> where harmonic force fields are obtained with fc-CCSD(T)/ANO2 level of theory while anharmonic force fields are calculated with fc-CCSD(T)/ANO1. The procedure used here for the ZPE differs from that in the standard HEAT protocol, which uses the cc-pVQZ basis set throughout, but was chosen here for computational cost consideration. In addition, other smaller corrections are also included: DBOC, spin-orbit correction, and scalar relativity effects. The CFOUR quantum chemical program<sup>35</sup> was used for all calculations.

Table 1 lists contributions of various terms to the heats of formation for  $C_2H_3$ ,  $C_2H_4$ , and  $C_2H_5$ . As is usual, the most important contribution is the SCF energy; the second most important is the

CCSD(T) electron correlation energy; and the third in magnitude is the ZPE. The remaining terms have small contributions, but including them is important to achieve the desired high level of accuracy. As observed here, heats of formation calculated with the HEAT-345Q method for these three species agree well (within  $0.5 \text{ kJ mol}^{-1}$ ) to those currently obtained from ATcT. It is expected that a similar accuracy is attained for other stationary points on the PES of the  $\text{C}_2\text{H}_5$  system.

### Statistical Kinetics Analysis

The reversible reactions (1, -1) are direct H-abstractions that do not pass through an energized intermediate, so they are pressure-independent. Thermal rate constants can be computed using transition state theory<sup>36, 37</sup> (i.e. at the high-pressure limit where the Boltzmann thermal energy distribution is fulfilled). For the forward reaction,  $\text{C}_2\text{H}_3 + \text{H}_2 \rightarrow \text{C}_2\text{H}_4 + \text{H}$ :

$$k(T)_1 = \frac{\sigma_1}{h} \cdot Q_t^\ddagger Q_e^\ddagger \cdot \frac{\sum_0^{J_{max}} (2J+1) \int_0^{E_{max}} G(E,J)_{rv}^\ddagger \exp(-E/RT) dE}{Q_{\text{C}_2\text{H}_3} Q_{\text{H}_2}} \quad (3)$$

where  $T$  is the reaction temperature,  $R$  is the gas constant,  $h$  is Planck's constant,  $Q_x$  is the complete partition function of species  $X$ ,  $Q_t^\ddagger$  and  $Q_e^\ddagger$  are the translational and electronic partition functions, respectively, for TS2, and  $\sigma_1$  is the reaction path degeneracy, which is equal to 2 (i.e. the rotational symmetry number of  $\text{H}_2$ ) in this case.  $J$  is the total angular momentum quantum number and  $E$  is the total internal energy.  $J_{max} = 300$  and  $E_{max} = 70,000 \text{ cm}^{-1}$  are chosen to ensure that the calculated  $k(T)$  converge for temperatures up to 4000 K. In this work,  $k(T)_1$  of Eq. 3 is computed numerically as a two-layer sum using  $\Delta J = 5$  and  $\Delta E = 10 \text{ cm}^{-1}$ .  $G(E,J)_{rv}^\ddagger$  is the sum of ro-vibrational states, which is obtained through convolution of (anharmonic) vibrational ( $G_v^\ddagger$ ) and rotational ( $\rho_r^\ddagger$ ) states:<sup>38-40</sup>

$$G_{rv}^{\ddagger}(E, J) = \sum_0^E G(E - E_r)_v^{\ddagger} \cdot \rho(E_r)_r^{\ddagger} \Delta E_r \quad (4)$$

$G_v^{\ddagger}$  is the (vibrational) cumulative reaction probability, as computed using Miller's semi-classical transition state theory (SCTST).<sup>41-45</sup> It should be mentioned that SCTST includes coupled anharmonic vibrations and multi-dimensional quantum mechanical tunneling effects within VPT2 theory.  $\rho_r^{\ddagger}$  is the density of (external) rotational states, and  $E_r$  is the rotational energy, which is given by Eq. 5 assuming that all stationary points are adequately approximated by a symmetric top:<sup>38, 46</sup>

$$E_r = \bar{B}J(J + 1) + (A - \bar{B})K^2 \text{ with } -J \leq K \leq +J \text{ and } \bar{B} = \sqrt{B \cdot C} \quad (5)$$

For the reverse reaction,  $C_2H_4 + H \rightarrow C_2H_3 + H_2$ , rate constants can be obtained via the thermal equilibrium condition when  $k(T)_1$  is known:

$$k(T)_{-1} = \frac{k(T)_1}{K(T)_{eq1}} \quad (6)$$

The reversible reactions,  $C_2H_4 + H \rightleftharpoons C_2H_5$  (2, -2), are obviously pressure-dependent, and a master-equation (ME) analysis<sup>47</sup> must be done to obtain phenomenological rate coefficients as functions of pressure and temperature. There are (at least) two different models<sup>47-53</sup> that can be used to obtain solutions in this case. If the forward reaction ( $C_2H_4 + H \rightarrow C_2H_5$ ) is considered, the ME model for a chemically activated reaction will be used.<sup>54</sup> If the reverse reaction ( $C_2H_5 \rightarrow C_2H_4 + H$ ) is the focus, the ME model for a thermally activated reaction will be applied.<sup>55</sup> The forward and reverse rate constants are again constrained by the thermal equilibrium constant,<sup>54, 56</sup> which does not depend on pressure.

$$k(T, P)_{-2} = \frac{k(T, P)_2}{K(T)_{eq2}} \quad (7)$$

To have a cross-check, both strategies mentioned above were used in this work; they pleasingly give essentially identical results. The main text will be based on the ME solution for the chemically activated reaction. Details of the other solution for the thermally activated reaction can be found in the Supplementary Material (SM).

An E,J-resolved two-dimensional master-equation<sup>14, 57-60</sup> that describes the time evolution for a competition of unimolecular dissociation of C<sub>2</sub>H<sub>5</sub> and energy transfer processes through collisions of vibrationally excited C<sub>2</sub>H<sub>5</sub> and a third body (i.e. bath gas) is expressed as:

$$\frac{\partial C_1(E_i J_i, t)}{\partial t} = \sum_{J_k=0}^{J_{max}} \int_{E_k=0}^{E_{max}} \omega_{LJ} \cdot P(E_i J_i | E_k J_k) \cdot C_1(E_k J_k, t) \cdot dE_k - \omega_{LJ} \cdot C_1(E_i J_i, t) - k_{1 \rightarrow 2}(E_i J_i) \cdot C_1(E_i J_i, t) + OST(E_i J_i) \quad (8)$$

where  $J_{max}$  is the maximum angular momentum;  $E_{max}$  is the maximum internal energy;  $C_1(E_i J_i, t)$  represents the population of C<sub>2</sub>H<sub>5</sub> in state  $(E_i J_i)$  and time  $t$ ;  $\omega_{LJ}$  (in  $s^{-1}$ ) is the Lennard-Jones collisional frequency,<sup>61-63</sup> and  $k_{1 \rightarrow 2}(E_i J_i)$  (in  $s^{-1}$ ) is the  $(E_i J_i)$ -resolved microcanonical rate coefficient from C<sub>2</sub>H<sub>5</sub> to C<sub>2</sub>H<sub>4</sub> + H. For the dissociation of C<sub>2</sub>H<sub>5</sub> via TS1, semiclassical TST (SCTST) theory is used to compute the microcanonical rate constants excluding angular momentum effects,  $k(E, J=0)$ . Rotational effects are then included using the J-shifting approximation,<sup>46, 64, 65</sup> assuming an active K-rotor model for both C<sub>2</sub>H<sub>5</sub> and TS1 (see Eq. 4). In Eq. 8,  $P(E_i J_i | E_k J_k)$  is the E,J-resolved collisional transfer probability distribution function from state  $(E_k J_k)$  to state  $(E_i J_i)$ . OST stands for the original source term, and is given by:<sup>39, 40, 66, 67</sup>

$$OST(E_i J_i) = F_{C_2H_5}(E_i J_i) \cdot k_2(T, \infty) \cdot [H] \cdot [C_2H_4]_0, \quad (9)$$

where  $k_2(T, \infty)$  is the *capture rate constant* for the association step (of H and C<sub>2</sub>H<sub>4</sub>) leading to population in the C<sub>2</sub>H<sub>5</sub> well.  $F_{C_2H_5}(E_i J_i)$  is the E,J-resolved initial distribution function for the nascent energized C<sub>2</sub>H<sub>5</sub> and is given by:<sup>39, 40, 66, 67</sup>

$$F_{C_2H_5}(E_i J_i) = \frac{(2J_i + 1) \cdot k_{1 \rightarrow 2}(E_i J_i) \cdot \rho_1(E_i J_i) \cdot \exp(-E_i/RT)}{\sum_{J_i=0}^{J_i^{max}} (2J_i + 1) \int_{E_i=0}^{E_i^{max}} k_{1 \rightarrow 2}(E_i J_i) \cdot \rho_1(E_i J_i) \cdot \exp(-E_i/RT) \cdot dE_i} \quad (10)$$

In Eq. (10),  $\rho_1(E_i J_i)$  is the density of rovibrational states for C<sub>2</sub>H<sub>5</sub>, for which the effects of anharmonicity are included in the approach followed here.

In the numerical calculations, an energy-grained master-equation is frequently used, with the result that the integral in Eq. 8 (of energy) becomes a sum. Therefore, Eq. 8 can be re-written as:

$$\frac{\partial C_1(E_i J_i, t)}{\partial t} = \sum_{J_k=0}^{J_k^{max}} \sum_{E_k=0}^{E_k^{max}} \omega_{LJ} \cdot P(E_i J_i | E_k J_k) \cdot C_1(E_k J_k, t) \cdot \Delta E - \omega_{LJ} \cdot C_1(E_i J_i, t) - k_{1 \rightarrow 2}(E_i J_i) \cdot C_1(E_i J_i, t) + OST(E_i J_i) \quad (11)$$

Eq. 11 can be cast in the matrix form:

$$\frac{\partial \mathbb{C}}{\partial t} = \mathbb{M} \mathbb{C} + R \cdot \mathbb{F}, \quad (12)$$

where  $\mathbb{C}$  represents the vector of population density for C<sub>2</sub>H<sub>5</sub>;  $\mathbb{M}$  denotes the transition matrix; R is a constant that is proportional to the capture rate constant,  $k_2(T, \infty)$ ; and  $\mathbb{F}$  is the vector comprising the E,J-resolved initial distribution function for the nascent energized C<sub>2</sub>H<sub>5</sub>.

Assuming the steady-state condition,<sup>66</sup>  $\partial \mathbb{C} / \partial t = 0$ , this leads to:

$$\frac{\partial \mathbb{C}_{SS}}{\partial t} = \mathbb{M} \mathbb{C}_{SS} + R \cdot \mathbb{F} = 0 \quad (13)$$

From Eq. 13,  $\mathbb{C}_{SS}$  is then obtained as:

$$\mathbb{C}_{SS} = -\mathbb{M}^{-1} \cdot R \cdot \mathbb{F} \quad (14)$$

The rate constant (in cm<sup>3</sup>/s) for each product channel is then calculated as (with  $R = k_2(T, \infty)$ ):

$$k_i(T,P) = \sum_{J=0}^{J_{max}} \sum_E^{E_{max}} k_i(E,J) \cdot C_i^{SS}(E,J), \quad (15)$$

and the product yield for each channel can be obtained from

$$\gamma_i(T,P) = k_i(T,P)/k_2(T,\infty). \quad (16)$$

It should be mentioned that the steady-state approximation works very well here when the temperature is  $\leq 800$  K: that is, when the thermal dissociation of (stabilized)  $C_2H_5$  remains slow or the re-activation process of thermalized  $C_2H_5$  is negligibly slow. When  $T \geq 1000$  K, the re-activation process of  $C_2H_5$  becomes fast enough that the steady-state solution eventually breaks down. In such a case, a time-dependent solution of the ME must be performed. In this work, the method proposed earlier by Pilling and coworkers has been used.<sup>54, 67</sup> As the H-atom is very reactive, [H] is assumed to be much smaller than  $[C_2H_4]$ , as one also assumes experimentally. As a result,  $[C_2H_4]$  remains almost unchanged when reacting with H-atoms. In this scenario, the decay of H is a (pseudo) first-order reaction with a microcanonical rate constant (from H to  $C_2H_5$ ) given by:  $k_{H \rightarrow C_2H_5}(E,J) = k_2(T,\infty) \cdot [C_2H_4]_0 \cdot F_{C_2H_5}(E,J)$ . To take this into account, the relaxation matrix  $\mathbb{M}$  with a dimension of  $(m)$  must be modified to a new and expanded matrix  $\mathbb{M}'$ . In the matrix  $\mathbb{M}'$ , each element of the  $(m+1)^{th}$  column is equal to  $k_{H \rightarrow C_2H_5}(E,J)$ , except the last element at the bottom-right. The last element  $(m+1,m+1)$  on the diagonal of  $\mathbb{M}'$  is given by  $-\sum_J \sum_E k_{H \rightarrow C_2H_5}(E,J) = -k_2(T,\infty) \cdot [C_2H_4]_0$ . In addition, each element of the associated  $(m+1)^{th}$  row vector represents the reverse microcanonical rate constant,  $k_{C_2H_5 \rightarrow H}(E,J)$ . It should be mentioned that there is an important property of this model: the sum of all elements of any column of the matrix  $\mathbb{M}'$  must be zero according to the law of conservation of mass.

The structure of this matrix  $\mathbb{M}'$  is given by:

$$\mathbb{M}' \equiv \begin{pmatrix}
 \mathbb{M}_{1,1} & \mathbb{M}_{1,2} & \mathbb{M}_{1,3} & & & \mathbb{M}_{1,m-1} & \mathbb{M}_{1,m} & k_2(\infty)[C_2H_4]_o F(E,1) \\
 \mathbb{M}_{2,1} & \mathbb{M}_{2,2} & \mathbb{M}_{2,3} & \dots\dots & & \mathbb{M}_{2,m-1} & \mathbb{M}_{2,m} & k_2(\infty)[C_2H_4]_o F(E,2) \\
 \mathbb{M}_{3,1} & \mathbb{M}_{3,2} & \mathbb{M}_{3,3} & & & \mathbb{M}_{3,m-1} & \mathbb{M}_{3,m} & k_2(\infty)[C_2H_4]_o F(E,3) \\
 & \vdots & & \ddots & & & & \vdots \\
 \mathbb{M}_{m-2,1} & \mathbb{M}_{m-2,2} & \mathbb{M}_{m-2,3} & & & \mathbb{M}_{m-2,m-1} & \mathbb{M}_{m-2,m} & k_2(\infty)[C_2H_4]_o F(E,m-2) \\
 \mathbb{M}_{m-1,1} & \mathbb{M}_{m-1,2} & \mathbb{M}_{m-1,3} & \dots\dots & & \mathbb{M}_{m-1,m-1} & \mathbb{M}_{m-1,m} & k_2(\infty)[C_2H_4]_o F(E,m-1) \\
 \mathbb{M}_{m,1} & \mathbb{M}_{m,2} & \mathbb{M}_{m,3} & & & \mathbb{M}_{m,m-1} & \mathbb{M}_{m,m} & k_2(\infty)[C_2H_4]_o F(E,m) \\
 k_{1 \rightarrow 2}(E,1) & k_{1 \rightarrow 2}(E,2) & k_{1 \rightarrow 2}(E,3) & & & k_{1 \rightarrow 2}(E,m-1) & k_{1 \rightarrow 2}(E,m) & -k_2(\infty)[C_2H_4]_o
 \end{pmatrix} \tag{17}$$

For off-diagonal submatrices of the matrix  $\mathbb{M}'$ :

$$\mathbb{M}_{J_y J_x} = \begin{pmatrix}
 P(1J_y|1J_x) & P(1J_y|2J_x) & & & P(1J_y|m-1J_x) & P(1J_y|mJ_x) \\
 P(2J_y|1J_x) & P(2J_y|2J_x) & \dots\dots & & P(2J_y|m-1J_x) & P(2J_y|mJ_x) \\
 & \vdots & & \ddots & & \vdots \\
 P(m-1J_y|1J_x) & P(m-1J_y|2J_x) & & & P(m-1J_y|m-1J_x) & P(m-1J_y|mJ_x) \\
 P(mJ_y|1J_x) & P(mJ_y|2J_x) & \dots\dots & & P(mJ_y|m-1J_x) & P(mJ_y|mJ_x)
 \end{pmatrix} \tag{18}$$

Each element of the small matrix  $\mathbb{M}_{J_y J_x}$  represents an E,J-resolved (normalized) collisional transfer probability.

For the diagonal submatrices:

$$\mathbb{M}_{JJ} = \begin{pmatrix}
 A(1|1)_J & A(1|2)_J & & & A(1|m-1)_J & A(1|m)_J \\
 A(2|1)_J & A(2|2)_J & \dots\dots & & A(2|m-1)_J & A(2|m)_J \\
 & \vdots & & \ddots & & \vdots \\
 A(m-1|1)_J & A(m-1|2)_J & & & A(m-1|m-1)_J & A(m-1|m)_J \\
 A(m|1)_J & A(m|2)_J & \dots\dots & & A(m|m-1)_J & A(m|m)_J
 \end{pmatrix} \tag{19}$$

Elements of the matrix  $\mathbb{M}_{JJ}$  are exactly like those in the 1DME scenario<sup>67</sup> and are given below:

For diagonal elements of the matrix  $\mathbb{M}_{JJ}$ :

$$A(i|i)_J = -k_{1 \rightarrow 2}(E_{ij}) - \omega_{LJ} + \omega_{LJ} \cdot P(iJ | iJ),$$

and for off-diagonal elements:

$$A(k|l)_J = P(k,J|l,J)$$

When  $[C_2H_4]$  is treated as constant, the reversible reaction  $C_2H_4 + H \rightleftharpoons C_2H_5$  here behaves like a reversible isomerization process,<sup>54, 68</sup> in which there are two low (chemically significant) eigenvalues:  $\lambda_1 = 0$  and  $-\lambda_2 = k_2[C_2H_4]_0 + k_{-2}$ . In addition,  $k_2$  and  $k_{-2}$  are coupled by the thermal equilibrium in Eq. 7. From these, both  $k_2$  and  $k_{-2}$  are given by:

$$k_2 = \frac{K_{eq2}}{1 + K_{eq2} \cdot [C_2H_4]_0} \cdot |\lambda_2|, \text{ in } cm^3 s^{-1},$$

$$k_{-2} = \frac{1}{1 + K_{eq2} \cdot [C_2H_4]_0} \cdot |\lambda_2|, \text{ in } s^{-1}. \quad (20)$$

In this work, the ARPACK software package<sup>69</sup> was used to find the two small eigenvalues  $\lambda_1$  and  $\lambda_2$  of the matrix  $M'$ , which are well separated from the rest of the spectrum (by a few orders of magnitude). The LAPACK software package<sup>70, 71</sup> that gives a full set of eigenvalues and eigenvectors was also used to check the solutions for manageable matrix sizes.

Considering the practical application of the model, air (i.e. a mixture of *ca.* 80% for  $N_2$  and *ca.* 20% for  $O_2$ ) is chosen as the bath gas. All collisional parameters and energies used in the E,J-resolved 2DME are listed in Table 2. The average downward energy transfer is considered as a function of temperature and given by Eq. 21, which is very similar to the form previously proposed by Miller and Klippenstein.<sup>55</sup> Given the lack of information regarding rotational energy transfer, the value of  $\langle \Delta E_d \rangle_{rot}$  is simply chosen to be the same as  $\langle \Delta E_d \rangle_{vib}$ .

$$\langle \Delta E_d \rangle_{vib} = \langle \Delta E_d \rangle_{rot} = 70 \cdot \left( \frac{T}{298} \right)^{0.94}, (\text{in } cm^{-1}) \text{ for the E,J-resolved 2DME model;}$$

$$\langle \Delta E_d \rangle_{vib} = 80 \cdot \left( \frac{T}{298} \right)^{0.94}, (\text{in } cm^{-1}) \text{ for the fixed-J 2DME model.} \quad (21)$$

As seen in Eq. 21,  $\langle \Delta E_d \rangle_{vib}$  depends on a ME model used as found recently.<sup>72</sup> It is usually found that the best choice of  $\langle \Delta E_d \rangle_{vib}$  for the fixed-J 2DME model is (slightly) larger than the E,J-resolved 2DME. It is also worth pointing out that the solution of the fixed-J 2DME model<sup>16-18, 73-75</sup> is a simplification of the E,J-resolved 2DME model<sup>14</sup> in which effects of the rotational energy transfer are completely neglected (i.e.  $\langle \Delta E_d \rangle_{rot} = 0$ ).<sup>14</sup>

## RESULTS and DISCUSSION

### ATcT Enthalpies of Formation

For the sake of completeness, Table 3 lists the ATcT enthalpies of formation of all  $C_2H_n$  ( $n = 6 - 0$ ) species. The discussion that follows focuses on the three  $C_2H_n$  species of relevance here, namely ethene, vinyl, and ethyl.

Perhaps not surprisingly, the thermochemistry of ethene was experimentally determined reasonably well early on. Since the calorimetric determination by Rossini and Knowlton<sup>76</sup> in the late 1930s, its enthalpy of formation underwent only minor revisions with the passage of time (see Table 4 for a list of historical values).<sup>77-90</sup> Earlier,<sup>91</sup> ATcT produced a 298.15 K value of  $52.45 \pm 0.13 \text{ kJ mol}^{-1}$  (or  $60.96 \pm 0.13 \text{ kJ mol}^{-1}$  at 0 K) using a significantly smaller TN (ver. 1.122). The current 298.15 K ATcT enthalpy of formation of ethene reflects further refinements and expansions of the TN and is the most accurate so far,  $\Delta_f H^\circ_{298}(C_2H_4) = 52.38 \pm 0.11 \text{ kJ mol}^{-1}$  ( $60.89 \pm 0.11 \text{ kJ mol}^{-1}$  at 0 K). Though technically any and all determinations included in the TN contribute to some degree to all resulting enthalpies of formation, the ATcT variance decomposition analysis<sup>92</sup> sheds a more quantitative light on the provenance of individual values.

In general, highly distributed provenances indicate that the resulting enthalpy of formation is quite robust, in the sense that it does not strongly depend on any single determination (in contrast to values obtained by traditional sequential thermochemistry). The variance decomposition indicates that the provenance of the enthalpy of formation of ethene is both heavily tilted toward experimental determinations and is extremely highly distributed. Namely, it would take no less than 866 various determinations extant in the TN to detail the top 90% of its pedigree, with the top contributor – combustion calorimetry of Rossini and Knowlton<sup>76</sup> – being responsible for no more than 9.3 % of the provenance.

The current ATcT enthalpy of formation of vinyl radical,  $\Delta_f H^\circ_{298}(\text{C}_2\text{H}_3) = 297.22 \pm 0.30 \text{ kJ mol}^{-1}$  ( $301.26 \pm 0.30 \text{ kJ mol}^{-1}$  at 0 K), is also rather similar to the previously published ATcT value<sup>92</sup> of  $296.91 \pm 0.33 \text{ kJ mol}^{-1}$  at 298.15 K ( $301.11 \pm 0.33 \text{ kJ mol}^{-1}$  at 0 K). Many of the earlier 298.15 K values<sup>92-95</sup> (see Table 4), though significantly less accurate, appear congruent with the current ATcT value, the most prominent exception being the significantly lower value originally recommended by Gurvich et al.<sup>88</sup> The ATcT variance decomposition analysis indicates that the provenance of the current enthalpy of formation of vinyl is rather highly distributed, albeit somewhat less than that of ethene: it would take 244 various determinations extant in the TN to detail the top 90% of its pedigree. Interestingly, although the provenance is dominated by results from very-high-level composite theoretical methods (such as W4,<sup>96-98</sup> HEAT,<sup>99</sup> ANL1<sup>100</sup>, and others<sup>101</sup>), the top contributor (5.3 %) is nevertheless an experimental determination (hydrogen abstraction of ethene by chlorine atoms<sup>102</sup>).

In contrast to the enthalpies of formation of ethene and vinyl, the enthalpy of formation of ethyl radical has a curiously checkered history (see Table 4). Both the NBS Tables<sup>80</sup> and Gurvich et al.<sup>88</sup>

provided similar 298.15 K values:  $107.5 (\pm 4.0)$  and  $107 \pm 6$  kJ mol<sup>-1</sup>, respectively. A subsequent photoionization study of the adiabatic ionization energy of ethyl radical<sup>103</sup> has indicated that these values are too low, and suggested a significantly higher value ( $\sim 119$  kJ mol<sup>-1</sup> at 298.15 K). This was further confirmed by kinetic studies that resulted in similarly higher 298.15 K values, such as  $121.0 \pm 1.5$  kJ mol<sup>-1</sup> (Seakins et al.<sup>104</sup>) and  $120.2 \pm 0.9$  kJ mol<sup>-1</sup> (Hanning-Lee et al.<sup>54</sup>), as well as the value of  $119 \pm 2$  kJ mol<sup>-1</sup> from the evaluation of kinetic data (Tsang<sup>95</sup>). A recent comprehensive photoionization study using isodesmic reaction networks (Bödi et al.<sup>105</sup>) also resulted in a similar 298.15 K value of  $120.7 \pm 1.1$  kJ mol<sup>-1</sup>. On the other hand, an even more recent kinetic study of bromination (Leplat et al.<sup>106</sup>) resulted in a somewhat lower 298.15 K value of  $117.3 \pm 3.1$  kJ mol<sup>-1</sup>, albeit with a sufficiently large uncertainty to provide some overlap with the other, nominally larger, kinetic values.

The current ATcT enthalpy of formation of ethyl radical is  $\Delta_f H^\circ_{298}(\text{C}_2\text{H}_5) = 120.63 \pm 0.22$  kJ mol<sup>-1</sup> ( $131.38 \pm 0.22$  kJ mol<sup>-1</sup> at 0 K). The most recent theoretical and experimental kinetic study, by Blitz et al.,<sup>107</sup> which focuses on the recombination of ethene with H-atoms and ethyl radical re-dissociation and appeared as we were composing the current manuscript (and was thus not included in the ATcT TN), suggests an enthalpy of formation of ethyl of  $120.49 \pm 0.57$  kJ mol<sup>-1</sup> at 298.15 K, nominally in superb agreement with the ATcT value, the two apparently independently confirming each other. The variance decomposition indicates that the provenance of the enthalpy of formation of ethyl is rather distributed, necessitating no less than 502 determinations to explain 90% of the provenance. It also signals that the provenance is dominated by experimental determinations, most of which are based on kinetic measurements at elevated temperatures. The top two contributors (15.8 % and 4.3 %) are the 3<sup>rd</sup> law free energies of the

C–H dissociation of ethyl determined by Brouard et al.<sup>108</sup> at two different temperatures, and the third (2.6 %) is the equilibrium constant of a bromination reaction determined from kinetic measurements.<sup>109, 110</sup> It should be mentioned here that although the 0 K values agree within their combined uncertainties, the current ATcT value for ethyl effectively supersedes the previously reported<sup>91</sup> value of  $119.86 \pm 0.28 \text{ kJ mol}^{-1}$  at 298.15 K ( $130.92 \pm 0.28 \text{ kJ mol}^{-1}$  at 0 K). Namely, the latter was obtained by using internally thermophysical properties that were corrected for the CH<sub>3</sub> torsion by folding in the rotation-torsion contribution via a state count over level energies obtained by combining computed levels with a set of experimental levels determined by Sears et al.<sup>111</sup> (which, by itself, was a significant improvement over the previous set of thermophysical properties, imported into ATcT directly from the TRC Tables<sup>86</sup>). The thermophysical properties are used by ATcT when constructing the TN to convert reaction enthalpies and/or free energies (specified initially at actual experimental temperatures) to a common temperature of the TN (298.15 K, in this case). As it turns out, in the case of ethyl, the majority of the relevant experimental determinations are at elevated temperatures and a proper account of anharmonic effects during the related temperature conversions is quite important, as anharmonic effects tend to become more prominent as the temperature increases.<sup>112</sup> The current ATcT value for ethyl makes use of refurbished thermophysical quantities that are entirely based on a nonrigid rotor anharmonic oscillator (NRRAO) partition function, obtained by a general approach outlined earlier,<sup>22, 25, 77</sup> a detailed account of which would be beyond the scope of the present work and will be discussed in a separate report.

The resulting ATcT C–H 0 K bond dissociation energy of ethene producing vinyl,  $D_0(\text{H–CHCH}_2) = 456.41 \pm 0.28 \text{ kJ mol}^{-1}$ , and the equivalent 298.15 K bond dissociation enthalpy is  $\text{BDE}_{298}(\text{H–}$

$\text{CHCH}_2) = 462.84 \pm 0.28 \text{ kJ mol}^{-1}$ . The 0 K bond dissociation energy and 298.15 K bond dissociation enthalpy of ethyl producing ethene,  $D_0(\text{H}-\text{CH}_2\text{CH}_2) = 145.54 \pm 0.20 \text{ kJ mol}^{-1}$  and  $\text{BDE}_{298}(\text{H}-\text{CH}_2\text{CH}_2) = 149.75 \pm 0.20 \text{ kJ mol}^{-1}$ , are, as expected, significantly lower, since in this case the removal of the H atom is compensated by strengthening the C–C bond from an essentially single bond in ethyl to a canonical C=C double bond in ethene, as discussed previously.<sup>91</sup> Both bond dissociation energies, together with the current ATcT values for the other bond dissociations in the  $\text{C}_2\text{H}_n$  system, are for convenience summarized in Table 5.

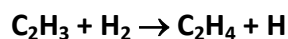


Figure 1 shows the PES calculated with the HEAT-345Q method. In addition, the results obtained by Schaefer and coworkers<sup>113</sup> using the conceptually similar Focal Point (FP) method, and those obtained from ATcT are included for the purpose of comparison. The reaction is exothermic by  $-24.34 \pm 0.29 \text{ kJ mol}^{-1}$  at 0 K, per ATcT. The HEAT and FP calculations give  $-24.8 \text{ kJ mol}^{-1}$  and  $-23.6 \text{ kJ mol}^{-1}$ , respectively, both in excellent agreement with ATcT (straddling the latter value by  $0.5 \text{ kJ mol}^{-1}$  on the low side and  $0.7 \text{ kJ mol}^{-1}$  on the high side). The barrier calculated with HEAT is  $39.1 \text{ kJ mol}^{-1}$ ,  $1.3 \text{ kJ mol}^{-1}$  lower than that predicted by FP method. From the Arrhenius expression,  $k(T)_1 = (3.42 \pm 0.35) \times 10^{-12} \times \exp(- (4179 \pm 67 \text{ K})/T)$ , fitted from experimental results in the temperature range of 499–947 K,<sup>4</sup> an activation energy of  $34.8 \pm 0.6 \text{ kJ mol}^{-1}$  can be derived. It should be noted that the experimental activation energy determined in this way is often too low for reactions involving significant displacement of hydrogen atoms because the experimental rate constants inherently include tunneling effects that bias the measured and effective activation energy to lower values.

Figure 2 shows the thermal rate constants calculated with SCTST theory (i.e. Eq. 3 above). Two experimental results were also included for comparison. The theoretical values from first-principles in this work agree well (within 20%) with the (direct) experimental results of Knyazev et al.,<sup>4</sup> but underestimate (indirect) experimental results<sup>6</sup> in the low temperature regime. One should note that the latter values from the indirect measurement have a high uncertainty.<sup>6</sup> By adjusting the ab initio barrier by  $-0.5 \text{ kJ mol}^{-1}$  (e.g. certainly well within possible error for the HEAT method), we are able to reproduce all experimental results of Knyazev et al.<sup>4</sup> This is remarkable, considering the simple formalism and practical applicability of SCTST theory. It is possible that an improved treatment of tunneling could lessen the gap between experiment and theory in the low temperature regime.

Tunneling effects were computed, and are displayed in Figure 3. The tunneling enhancement steeply decreases when temperature increases, as expected. It is about 3.84 at 300 K, dropping quickly to 1.64 at 500 K, and then to 1.15 at 1000 K. It differs negligibly from unity at higher temperatures. Because of this, tunneling effects are relatively unimportant in the experiment of Knyazev et al.<sup>4</sup>



The reverse reaction (–1) has a high barrier of  $63.9 \text{ kJ mol}^{-1}$  (see Figure 1), so it cannot compete with the lower-lying H-addition path (2, see below) in the low temperature regime ( $T < 1000 \text{ K}$ ), but is expected to play an important role at high combustion temperatures ( $T \geq 1000 \text{ K}$ ). Given that both the H-abstraction and H-addition pathways can occur in parallel and are in competition with each other at high temperature, direct measurements of rate constants (e.g. via the decay

of H atom in experiment) are very challenging. As a result, there are no direct experimental results available for this reaction. Very recently, Davidson and coworkers<sup>5</sup> deduced rate constants from a shock tube experiment by matching the concentration profile of C<sub>2</sub>H<sub>4</sub> in their model with the measurement in a mixture of C<sub>2</sub>H<sub>4</sub>/CH<sub>4</sub>/H<sub>2</sub>/Ar at about 10 atm and in a temperature range of 1619–1948 K. Because of the indirect nature of the experiment, however, these rate constant measurements still have a fairly significant uncertainty of  $\pm 35\%$ .<sup>5</sup>

In this work, rate constants for the reverse reaction ( $k_{-1}$ ) of C<sub>2</sub>H<sub>4</sub> + H → C<sub>2</sub>H<sub>3</sub> + H<sub>2</sub> were computed using the thermal equilibrium constant ( $K_{\text{eq}1}$ ) together with the forward rate constant ( $k_1$ ) obtained above (see Eq. 6). Here,  $K_{\text{eq}1}$  was computed using the high accuracy reaction enthalpy of  $-24.34 \pm 0.29$  kJ mol<sup>-1</sup> from ATcT and partition functions, which were computed using ro-vibrational parameters and anharmonic constants from first principles. The calculated results are displayed in Figure 4, where experimental data are included for comparison. Inspection of the Figure shows that the calculated rate constants are in close agreement with all experimental results within the error bars.<sup>2, 5, 7-10</sup> As mentioned, the large experimental error bars are due to the indirect nature of the measurements.<sup>2, 5, 7-10</sup> The SCTST values appear to be slightly higher than those recommended by Baulch et. al.<sup>2</sup> at lower temperature, but become slightly lower at higher temperature. In addition, in the high temperature regime, the SCTST rate constants are in closer agreement with the experiment of Davidson and coworkers.<sup>5</sup> However, as compared to the experiment of Just et al.,<sup>7</sup> we underestimate the rate constants by a factor of about 2. This might be due to other pathways that might open at high temperature. Very recently, Bowman and coworkers<sup>114</sup> have found a roaming pathway for the direct H-abstraction from C<sub>2</sub>H<sub>4</sub> + H to C<sub>2</sub>H<sub>3</sub> + H<sub>2</sub> on the basis of dynamics calculations.<sup>114</sup> The roaming pathway was found to occur at a

high threshold of *ca.* 30 kcal mol<sup>-1</sup> (125.5 kJ mol<sup>-1</sup>), so it is likely to open only for very high collision energies.<sup>114</sup> It was also estimated that the contribution of the roaming channel was about 16% at a collision energy of 60 kcal mol<sup>-1</sup>.<sup>114</sup> Under the experimental conditions ( $T < 2000$  K), where much less collision energy is available, the roaming pathway is certain to be minor, with a likely contribution of less than 5%. So, the differences (e.g. a factor of 2) between the experiment of Just et. al.<sup>7</sup> and theory cannot be rationalized in this way. Further experimental work appears to be warranted.



This reaction plays an important role for the formation of C<sub>2</sub>H<sub>5</sub> in low temperature combustion. It is the simplest reaction for H-addition to a C=C double bond, and it is pressure-dependent; this process is therefore fundamentally both interesting and important.<sup>54, 55, 115-118</sup> As an example of how reactions of this type have an importance that extends well beyond this prototypical system, it may be instructive to point out how reactions of this type may play some role in soot formation. Fall-off curves for the reaction between H and C<sub>2</sub>H<sub>4</sub> were experimentally observed at low temperatures (285 to 800 K) and low-to-ambient pressures (1 to 760 Torr).<sup>54, 115, 117</sup> Theoretical results from a ME analysis have been reported,<sup>54, 55, 118</sup> and are in good agreement with experiment. There are no experimental data at higher temperatures where the direct H-abstraction pathway (see above) opens and can compete with the H-addition. Here we focus on the competition of these two pathways in the fall-off regime at high combustion temperatures. Figure 5 shows the PES of the C<sub>2</sub>H<sub>4</sub> + H ⇌ C<sub>2</sub>H<sub>5</sub> reaction constructed with HEAT-345Q method. The H-addition proceeds via TS1, facing a barrier of 12.2 kJ mol<sup>-1</sup>, leading to the formation of

vibrationally excited  $C_2H_5$ . This barrier height is in good agreement with a previous theoretical value of  $11.7 \text{ kJ mol}^{-1}$ .<sup>55</sup> The adduct ( $C_2H_5$ ) has a binding energy of  $-145.6 \text{ kJ mol}^{-1}$ , in excellent agreement with an ATcT value of  $-145.54 \pm 0.20 \text{ kJ mol}^{-1}$ .  $C_2H_5$ , when produced, can undergo an automerization step via TS3, which needs to overcome a barrier of  $167.0 \text{ kJ mol}^{-1}$ ; this is  $9.2 \text{ kJ mol}^{-1}$  higher than its re-dissociation step (via TS1) back to initial reactants,  $C_2H_4 + H$ . Moreover, TS3 is much tighter than TS1. As a result, the re-dissociation step is favored both energetically and entropically, as was predicted by Harding.<sup>119</sup> It is worth mentioning that including the automerization step does not change the outcome of the ME analysis, but doubles the size of the relaxation matrix. Note that we are unable to find a direct  $H_2$ -elimination pathway from  $C_2H_5$  (via a first-order saddle point) to  $C_2H_3 + H_2$ ; the same qualitative observation has been reported elsewhere.<sup>114, 120</sup>

Figures 6 and 7 show fall-off curves for H-addition below 800 K; experimental data (where available) are also included for comparison. As seen, we are able to reproduce experimental results for a wide range of temperature and pressure; these results imply that the PES and the ME model used here are reliable. Note that there is a low frequency vibration, which corresponds to the torsional mode in  $C_2H_5$ . In the current ME model, this torsion is assumed to be separable from the remaining vibrations and is treated as a 1D-hindered rotor. The 1D Schrodinger equation was solved to obtain a vector of (torsional) eigenvalues, which were then used to directly count the density of torsional states.<sup>47</sup> The overall density of states of  $C_2H_5$  was finally obtained by convolving that of the torsion and the other vibrations.

In the ME simulation, there is only one unknown parameter, specifically an average energy transferred per collision in a downward direction,  $\langle \Delta E_d \rangle$ . In this work, we (empirically) chose

$\langle \Delta E_d \rangle$  such that the calculated rate constants at 298 K match with experiment (see Figure 6).<sup>115</sup>

We obtained  $\langle \Delta E_d \rangle$  – depending on temperature – that is in very close agreement to the value reported by Miller and Klippenstein (see Eq. 21).<sup>55</sup> It should be noted that this selected value  $\langle \Delta E_d \rangle$  may have a small error bar (*ca.*  $\pm 10 \text{ cm}^{-1}$ ) because experimental data at 298 K are rather scattered<sup>115</sup> (see Figure 6).

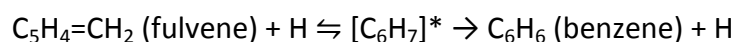
Figure 8 shows the complicated dependence of rate constant on temperature and pressure. It increases with pressure, as expected. The red solid line is the *capture* rate constant calculated at the high-pressure limit, leading to the formation of 100% thermalized  $\text{C}_2\text{H}_5$ ; and the thermal re-dissociation of  $\text{C}_2\text{H}_5$  is then assumed to be negligibly slow. This (simple) assumption is valid at low temperatures ( $T \leq 500 \text{ K}$ ), but breaks down at temperatures where the re-activation and thermal decomposition processes of  $\text{C}_2\text{H}_5$  become significantly faster. As a conspicuous result of this, the fall-off curves (as a function of temperature at a fixed pressure) pass through a maximum and decrease when temperature increases.

Figure 9 shows a comparison of the H-addition and H-abstraction pathways as functions of temperature and pressure. The H-abstraction is pressure-independent; thus, there is only one curve. In contrast, for the H-addition there are many (fall-off) curves due to its dependence on pressure. Overall, the H-abstraction increases with temperature while the H-addition decreases. At 10 atm (the pressure used in the experimental work of Davidson and coworkers<sup>5</sup>), the two curves cross at about 1650 K. Below that temperature, H-addition predominates; whereas the H-abstraction takes over at higher temperatures. Because of this competition, it is not easy to measure rate constants (directly) at high combustion temperature; it is obvious that both pathways must be included in a kinetic modeling of flames.

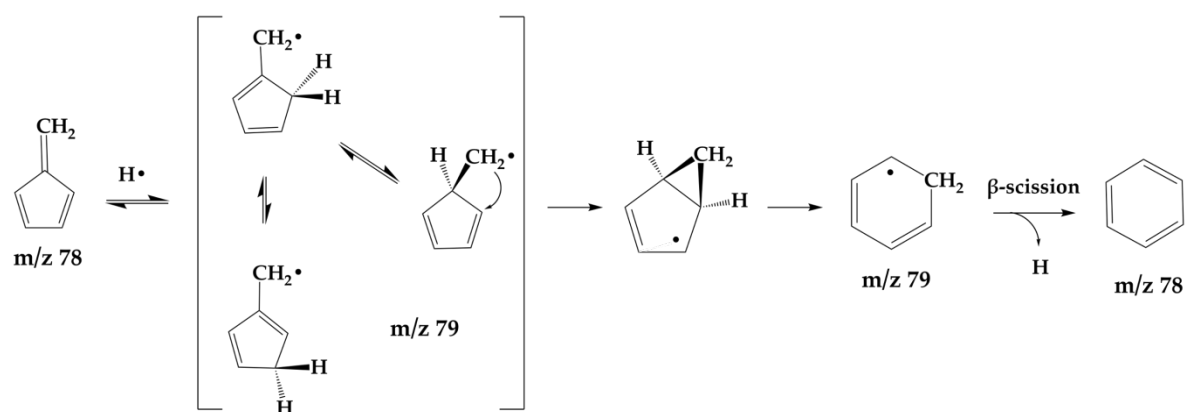
While this work was being prepared, a paper of Blitz et al.<sup>107</sup> on the  $C_2H_4 + H = C_2H_5$  reaction has appeared. In that report, Blitz et al. have used an 1D master equation technique to optimize a heat of formation of  $C_2H_5$  as well as other collisional energy transfer parameters by matching the calculated rate constants (in falloff regime) with available experimental data. The results obtained in this work agree well with those reported by Blitz et al. (see Table 6).

It is perhaps worthwhile to point out that reactions of this type have an importance that extends well beyond the prototypical  $H + C_2H_4$  system studied here. In hydrocarbon flames, pools of resonance-stabilized radicals rise to concentrations at which they combine with each other and form aromatic compounds. Some of these reactions produce extremely stable<sup>121</sup> polycyclic aromatic hydrocarbons (PAHs), while others grow larger resonance-stabilized radicals. The latter type of radical is hypothesized to be part of a chain reaction that quickly binds hydrocarbons together, eventually producing a product that is large enough to have the characteristics of a condensed-phase particle (i.e. incipient soot). This mechanism, in which resonance-stabilized-radical chain reactions lead to PAH growth and eventually soot inception, is the essence of the CHRCR mechanism proposed by Johansson *et al.*<sup>122</sup>

Many of these radical/radical reactions<sup>123-125</sup> are believed to form fulvene which isomerizes to benzene. There are two qualitatively different pathways for fulvene to isomerize to benzene. In addition to unimolecular fulvene isomerization,<sup>126</sup> there is a plausible bimolecular process that features catalytic H-atom addition/elimination.<sup>127</sup>



This has been called the H-assisted pathway,<sup>128, 129</sup> and starts with H-atom addition to the double bond followed by rearrangement. Recently the first experimental evidence<sup>130</sup> for the H-assisted pathway has been found in the radical/radical reaction:  $\text{CH}_3$  with  $\text{C}_5\text{H}_5 \rightarrow \text{C}_6\text{H}_6$  (benzene).



**Scheme 1:** Schematic reaction pathways for the H-assisted isomerization of fulvene to benzene.

Without H-assistance, the isomerization step occurs very slowly (even at high combustion temperatures) because it must overcome very high barriers.<sup>123, 131, 132</sup> Such a mechanism is likely to be generic in nature. The H-assisted isomerization from fulvene to benzene is a well-known example; and it has been verified by theoretical calculations<sup>127, 128</sup> but not yet confirmed experimentally.

## CONCLUSIONS

The thermochemistry, mechanism, and kinetics of the title reactions were studied using ATcT, high-level coupled cluster (HEAT), and E,J-resolved ME calculations. Some important results emerge from this work, which can be summarized as follows:

- 1) Heats of formation (all in  $\text{kJ mol}^{-1}$ ) for  $\text{C}_2\text{H}_3$ ,  $\text{C}_2\text{H}_4$ , and  $\text{C}_2\text{H}_5$  at 0 K (298 K) are respectively recommended to be  $\Delta H_{\text{C}_2\text{H}_3}^0 = 301.26 \pm 0.30$  ( $297.22 \pm 0.30$ ),  $\Delta H_{\text{C}_2\text{H}_4}^0 = 60.89 \pm 0.11$  ( $52.38 \pm 0.11$ ), and  $\Delta H_{\text{C}_2\text{H}_5}^0 = 131.38 \pm 0.22$  ( $120.63 \pm 0.22$ ), from the most current ATcT thermochemical network.
- 2) The calculated rate constants for  $\text{C}_2\text{H}_3 + \text{H}_2 \rightarrow \text{C}_2\text{H}_4 + \text{H}$  agree well with the direct measurement of Knyazev et. al.<sup>4</sup> in the temperature range of 499-947 K. We provide the theoretical results at  $T \geq 950$  K (Table S1 in the Supplementary Material) for kinetic modeling.
- 3) The calculated rate constants for  $\text{C}_2\text{H}_4 + \text{H} \rightarrow \text{C}_2\text{H}_3 + \text{H}_2$  agree closely (within the experimental uncertainty of  $\pm 35\%$ ) with the recent measurement of Davidson and coworkers,<sup>5</sup> but are smaller than the indirect experimental results of Just et. al.<sup>7</sup> Further experimental work is desirable in this regard.
- 4) The experimental fall-off results<sup>115, 117</sup> available in a low temperature regime for  $\text{C}_2\text{H}_4 + \text{H} + \text{M} \rightleftharpoons \text{C}_2\text{H}_5 + \text{M}$  are well replicated in the current work.
- 5) The H-abstraction and the H-addition pathways are in competition at high combustion temperature, rendering experimental characterization challenging. Thus, experimental data are lacking; and both pathways must be included in kinetic modeling. The high-level theoretical results are provided in Tables S2 to S6 in the Supplementary Material for that purpose.

### **Supplementary Material**

See the [supplementary material](#) for optimized geometries, ro-vibrational parameters, anharmonic constants, the calculated rate coefficients, and additional figures.

### **Acknowledgments**

This material is based on work supported by the U.S. Department of Energy, Office of Basic Energy Sciences under Award DE-SC0018164. The work at Argonne National Laboratory was supported by the U.S. Department of Energy, Office of Science, Office of Basic Energy Sciences, Division of Chemical Sciences, Geosciences and Biosciences, under Contract No. DE-AC02-06CH11357, through the Gas-Phase Chemical Physics Program (BR) and the Computational Chemical Sciences Program (DHB).

### **Data Available**

The data that support the findings of this study are available within the article and its [supplementary material](#). The data that support the findings of this study are available from the corresponding author upon reasonable request.

**Conflicts of Interest:** There are no conflicts of interest to declare.

**Table 1:** Individual contributions (kJ mol<sup>-1</sup>) of various terms to total atomization energies (TAE) and heats of formation (HFM) of C<sub>2</sub>H<sub>3</sub>, C<sub>2</sub>H<sub>4</sub> and C<sub>2</sub>H<sub>5</sub> (calculated at 0 K) using HEAT-345Q protocol.

Term	C <sub>2</sub> H <sub>3</sub>	C <sub>2</sub> H <sub>4</sub>	C <sub>2</sub> H <sub>5</sub>
δE <sub>SCF</sub>	1415.47	1794.03	1962.16
δE <sub>CCSD(T)</sub>	449.40	566.77	566.22
δE <sub>CCSDT</sub>	0.07	-2.01	-1.08
δE <sub>CCSDTQ</sub>	1.26	1.36	0.73
δE <sub>Scalar</sub>	-1.29	-1.38	-1.58
δE <sub>ZPE</sub>	-94.85	-131.76	-153.79
δE <sub>DBOC</sub>	0.12	0.22	0.17
δE <sub>Spin-orbit</sub>	-0.71	-0.71	-0.71
TAE	1769.47	2226.52	2372.11
HEAT	301.44 ± 0.5 <sup>a)</sup>	60.42 ± 0.5 <sup>a)</sup>	130.87 ± 0.5 <sup>a)</sup>
ATcT	301.26 ± 0.30 <sup>b)</sup>	60.89 ± 0.11 <sup>b)</sup>	131.38 ± 0.22 <sup>b)</sup>

- a) Heats of formation are derived from heats of formation at 0 K of H (216.034 ± 0.000 kJ mol<sup>-1</sup>) and C (711.404 ± 0.044 kJ mol<sup>-1</sup>), which are taken from ATcT using TN ver. 1.124.  
 b) Taken from ATcT TN ver. 1.124.

**Table 2:** Collisional parameters and energies are used in the E,J-resolved 2DME model.

Parameters	Values
Air (80% N <sub>2</sub> and 20% O <sub>2</sub> )	Mass = 28.8 g/mol, $\sigma = 3.668 \text{ \AA}$ , $\varepsilon/k_B = 86.2 \text{ K}^{1-2}$ )
C <sub>2</sub> H <sub>5</sub>	Mass = 29.06 g/mol, $\sigma = 4.31 \text{ \AA}$ , $\varepsilon/k_B = 225.5 \text{ K}^{1-2}$ )
E <sub>max</sub>	30,000 cm <sup>-1</sup> above C <sub>2</sub> H <sub>5</sub> when T ≤ 800 K; 60,000 cm <sup>-1</sup> above C <sub>2</sub> H <sub>5</sub> when T ≥ 1000 K.
ΔE <sub>grain</sub>	10 cm <sup>-1</sup> when T ≤ 800 K; and 30 cm <sup>-1</sup> when T ≥ 1000 K.
<ΔE <sub>d</sub> >	$80 \cdot \left(\frac{T}{298}\right)^{0.94}$ (in cm <sup>-1</sup> ), for the fixed-J ME model $70 \cdot \left(\frac{T}{298}\right)^{0.94}$ (in cm <sup>-1</sup> ), for the E,J-resolved ME model
J <sub>max</sub>	100 with T ≤ 800 K; and 200 with T ≥ 1000 K.
ΔJ	5

1) From Hippler et al.<sup>133</sup>

2) From the Multiwell software package.<sup>47</sup> In this work, the collisional parameters of C<sub>2</sub>H<sub>5</sub> were estimated as an average value of C<sub>2</sub>H<sub>4</sub> and C<sub>2</sub>H<sub>6</sub>.

**Table 3:** Enthalpies of formation,  $\Delta_f H^\circ$ , in  $\text{kJ mol}^{-1}$ , of  $\text{C}_2\text{H}_n$ ,  $n = 6-0$  species, based on ATcT TN ver.

1.124 of the TN.

Species	0 K	298.15 K	Uncert.
$\text{CH}_3\text{CH}_3$	-68.39	-84.02	$\pm 0.12$
$\text{CH}_3\text{CH}_2$	131.38	120.63	$\pm 0.22$
$\text{CH}_2\text{CH}_2$	60.89	52.38	$\pm 0.11$
$\text{CH}_3\text{CH}$	361.27	354.29	$\pm 0.46$
$\text{CH}_2\text{CH}$	301.26	297.22	$\pm 0.30$
$\text{CH}_3\text{C}$	508.60	504.90	$\pm 0.80$
$\text{CHCH}$	228.88	228.32	$\pm 0.13$
$\text{CCH}_2$	411.23	412.14	$\pm 0.30$
$\text{CCH}$	563.76	567.88	$\pm 0.15$
$\text{C}_2$	820.01	828.47	$\pm 0.10$

**Table 4.** Historical values for the 298.15 K enthalpies of formation of ethene, and vinyl and ethyl radical

$\Delta_f H^\circ(298.15 \text{ K})$ (kJ mol <sup>-1</sup> )	Reference
<b>C<sub>2</sub>H<sub>4</sub></b>	
52.5 ± 0.3	Rossini and Knowlton <sup>76</sup> 1937
52.28 (± 0.40)	Rossini et al. <sup>77</sup> 1947 Rossini et al. <sup>78</sup> 1952
52.26 (± 0.40)	NBS TN720 <sup>79</sup> 1968 NBS Tables <sup>80</sup> 1982
52.09 ± 0.40	Cox and Pilcher <sup>81</sup> 1970
52.47 ± 0.29	JANAF <sup>82</sup> 1971 JANAF <sup>83</sup> 1985 JANAF <sup>84</sup> 1998
52.51 ± 0.63	Chao and Zwolinski <sup>85</sup> 1975 TRC Tables <sup>86</sup> 1985
52.5 ± 0.4	Pedley et al. <sup>87</sup> 1986
52.4 ± 0.5	Glushko et al. <sup>88</sup> 1979 Gurvich et al. <sup>89</sup> 1990 Manion 2002 <sup>90</sup> 2002
52.45 ± 0.13	ATcT <sup>91</sup> 2015
52.38 ± 0.11	ATcT current value
<b>C<sub>2</sub>H<sub>3</sub></b>	
260 ± 10	Glushko et al. <sup>88</sup> 1979 Gurvich et al. <sup>89</sup> 1990
295 ± 7	Berkowitz et al. <sup>93</sup> 1988
300.0 ± 3.3	Ervin et al. <sup>94</sup> 1990
299 ± 5	Tsang <sup>95</sup> 1996
296.91 ± 0.33	ATcT <sup>91</sup> 2015
297.22 ± 0.30	ATcT current value
<b>C<sub>2</sub>H<sub>5</sub></b>	
107 ± 6	Glushko et al. <sup>88</sup> 1979 Gurvich et al. <sup>89</sup> 1990
107.5 (± 4.0)	NBS Tables <sup>80</sup> 1982
~119	Ruscic et al. <sup>103</sup> 1989
121.0 ± 1.5	Seakins et al. <sup>104</sup> 1992
120.2 ± 0.9	Hanning-Lee et al. <sup>54</sup> 1993
119 ± 2	Tsang <sup>95</sup> 1996
120.7 ± 1.1	Bödi et al. <sup>105</sup> 2006
117.3 ± 3.1	Leplat et al. <sup>106</sup> 2013
120.49 ± 0.57	Blitz et al. <sup>107</sup> 2021
119.86 ± 0.28	ATcT <sup>91</sup> 2015
120.63 ± 0.22	ATcT current value

**Table 5:** C-H and C-C bond dissociation energies and enthalpies (in  $\text{kJ mol}^{-1}$ ) in the  $\text{C}_2\text{H}_n$  system of species, based on ATcT TN ver. 1.124 of the TN.

Bond Dissociation	0 K	298.15 K	Uncert.
H-CH <sub>2</sub> CH <sub>3</sub>	415.81	422.65	± 0.20
H-CH <sub>2</sub> CH <sub>2</sub>	145.54	149.75	± 0.20
CH <sub>3</sub> CH-H	445.92	451.65	± 0.47
H-CHCH <sub>2</sub>	456.41	462.84	± 0.28
H-CH <sub>2</sub> CH	156.03	160.94	± 0.53
CH <sub>3</sub> C-H	363.37	368.61	± 0.91
H-CHCH	143.65	149.09	± 0.29
CH <sub>2</sub> C-H	326.00	332.92	± 0.37
H-CH <sub>2</sub> C	118.67	125.24	± 0.83
CHC-H	550.92	557.56	± 0.11
H-CHC	368.57	373.73	± 0.30
H-CC	472.28	478.59	± 0.13
CH <sub>3</sub> -CH <sub>3</sub>	368.14	376.96	± 0.13
CH <sub>3</sub> -CH <sub>2</sub>	409.54	417.44	± 0.23
CH <sub>2</sub> -CH <sub>2</sub>	721.22	730.82	± 0.20
CH <sub>3</sub> -CH	381.44	388.36	± 0.46
CH <sub>2</sub> -CH	682.63	690.55	± 0.32
CH <sub>3</sub> -C	352.68	358.46	± 0.80
CH-CH	956.80	964.03	± 0.20
CH <sub>2</sub> -C	691.23	696.35	± 0.30
CH-C	740.48	745.19	± 0.15
C-C	602.80	605.31	± 0.03

**Table 6:** A comparison of the results obtained in this work with those reported by Blitz et al (Ref. <sup>107</sup>)

Parameters	This work	Blitz et al (Ref. <sup>107</sup> )
$\Delta H_f$ (in $\text{kJ mol}^{-1}$ )	$131.38 \pm 0.22$ at 0 K ( $120.63 \pm 0.22$ at 298 K)	$131.55 \pm 0.57$ ( $120.49 \pm 0.57$ )
$\Delta H_r$ (in $\text{kJ mol}^{-1}$ )	$-145.54 \pm 0.20$	$-145.34 \pm 0.60$
$\Delta V_a$ (barrier, $\text{kJ mol}^{-1}$ )	$11.75 \pm 0.50$	$11.43 \pm 0.34$
$\omega_{\text{imag}}$ (in $\text{cm}^{-1}$ )	$730 \pm 20$ <sup>a)</sup>	$730 \pm 130$
$\langle \Delta E \rangle_{d,298K}$	$70 \pm 10 \text{ cm}^{-1}$ for air (80% $\text{N}_2$ and 20% $\text{O}_2$ )	$54.2 \pm 7.6 \text{ cm}^{-1}$ for He $62.2 \pm 5.5 \text{ cm}^{-1}$ for $\text{N}_2$

- a) This value is obtained by extrapolating to the complete basis set limit using  $\omega_{\text{imag}}^X = \omega_{\text{imag}}^\infty + \frac{a}{X^3}$ , where X = T and Q. The reaction coordinate vibrational frequencies are 756i, 719i, and 725i  $\text{cm}^{-1}$  calculated using fc-CCSD(T)/aVDZ, aVTZ, and aVQZ, respectively.

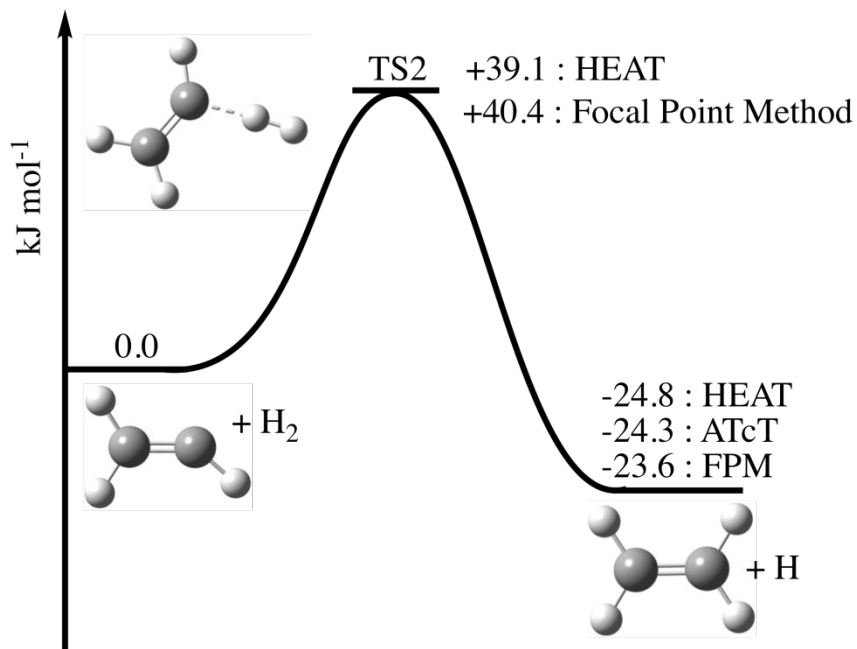


**Figure 1:** Schematic reaction energy profile for  $\text{C}_2\text{H}_3 + \text{H}_2 \rightarrow \text{C}_2\text{H}_4 + \text{H}$  calculated with HEAT-345Q method. Values from ATcT TN ver. 1.24 and Focal Point method (ref. <sup>113</sup>) are also included for comparison.

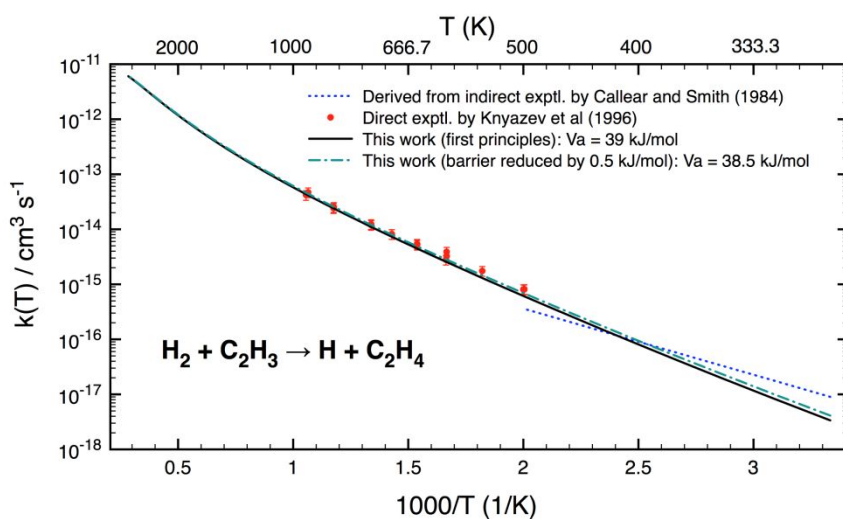


**Figure 2:** Rate constants as a function of temperature for the  $\text{C}_2\text{H}_3 + \text{H}_2 \rightarrow \text{C}_2\text{H}_4 + \text{H}$  reaction calculated using SCTST theory. Experimental data available are also included for comparison.

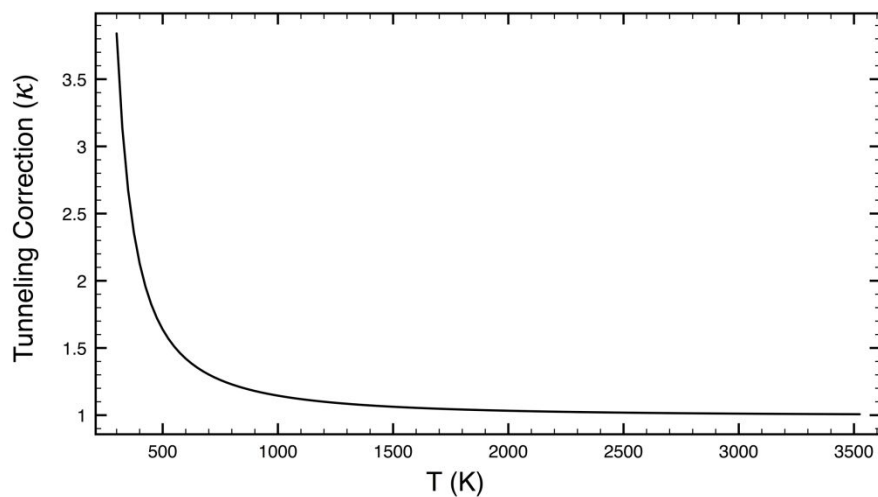


**Figure 3:** Multi-dimensional tunneling correction calculated as a function of temperature for the  $\text{C}_2\text{H}_3 + \text{H}_2 \rightarrow \text{C}_2\text{H}_4 + \text{H}$  reaction using SCTST method.

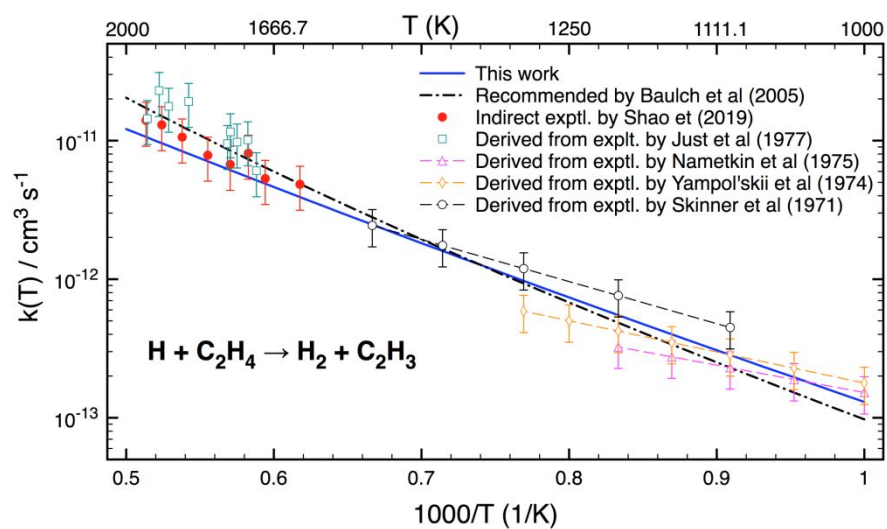


**Figure 4:** Rate constants for the  $\text{C}_2\text{H}_4 + \text{H} \rightarrow \text{C}_2\text{H}_3 + \text{H}_2$  reaction calculated as a function of temperature. Other data from literature are also included for comparison.

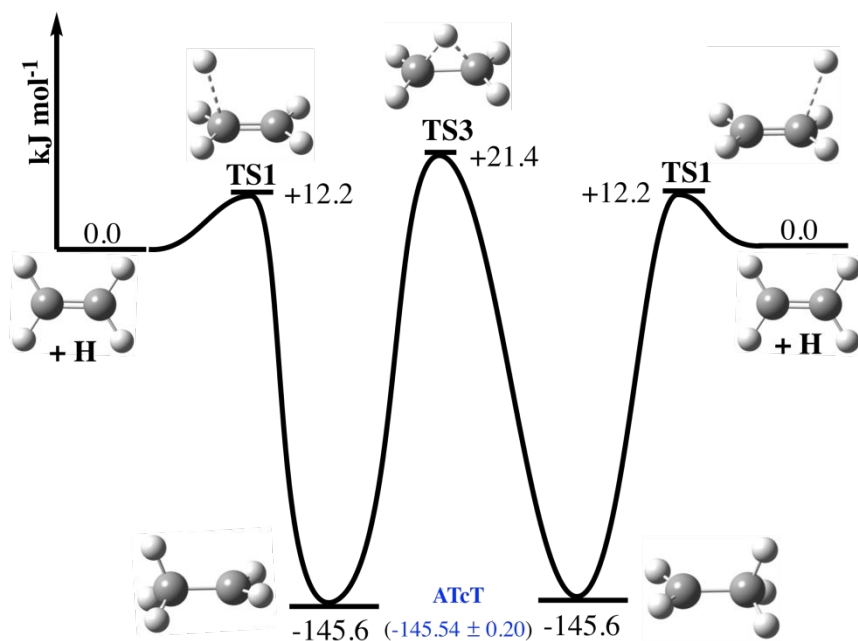


**Figure 5:** Schematic reaction energy profile for the reversible reaction of  $\text{C}_2\text{H}_4 + \text{H} \rightleftharpoons \text{C}_2\text{H}_5$  constructed using HEAT-345Q method.

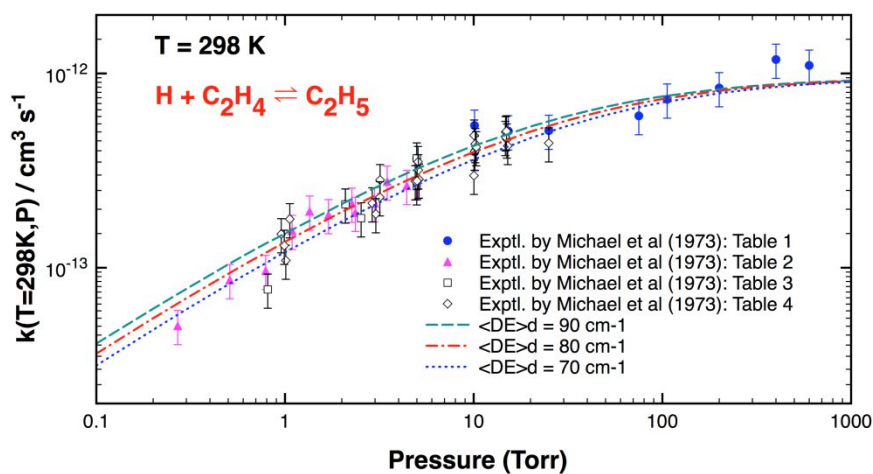


**Figure 6:** Fall-off curves calculated at 298 K for the  $\text{C}_2\text{H}_4 + \text{H} \rightleftharpoons \text{C}_2\text{H}_5$  reaction. Experimental data<sup>115</sup> are also included for comparison.

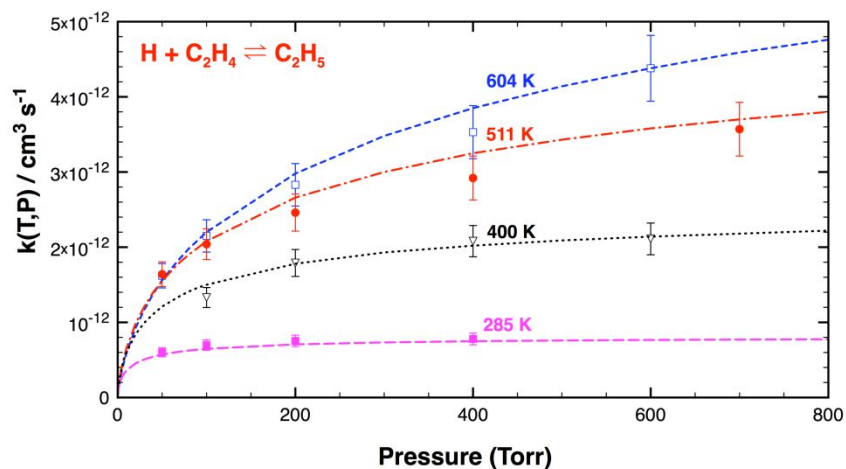


**Figure 7:** Fall-off curves for a wide low temperature and pressure calculated for the  $\text{C}_2\text{H}_4 + \text{H} \rightleftharpoons \text{C}_2\text{H}_5$  reaction. Experimental data<sup>117</sup> are also included for comparison.

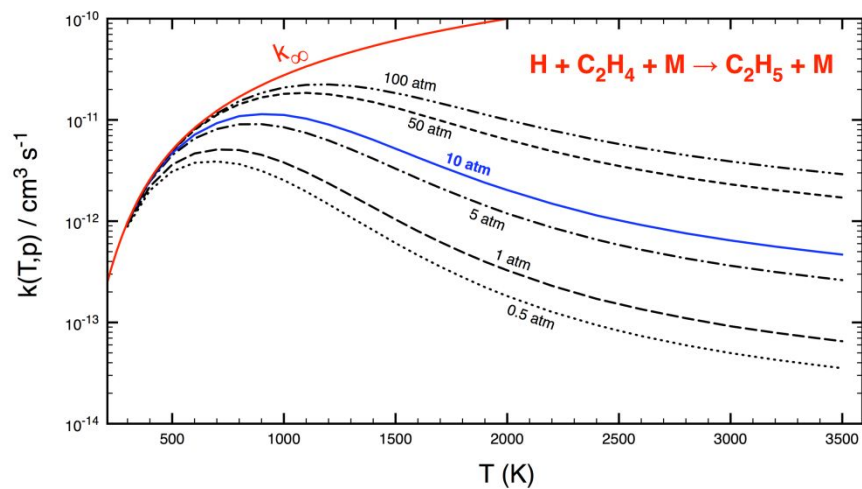


**Figure 8:** Rate constants as functions of temperature and pressure calculated for the  $\text{C}_2\text{H}_4 + \text{H} \rightleftharpoons \text{C}_2\text{H}_5$  reaction.

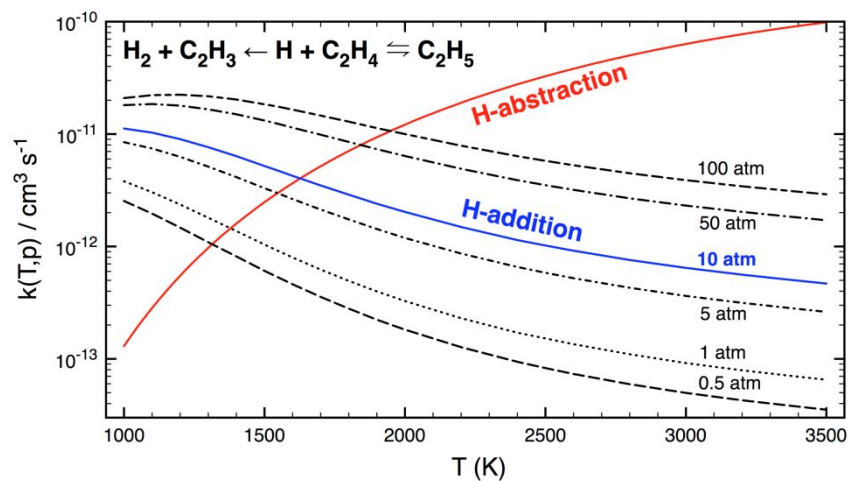


**Figure 9:** A comparison of the calculated rate constants for the H-abstraction and the-addition pathways in the  $\text{C}_2\text{H}_3 + \text{H}_2 \leftarrow \text{C}_2\text{H}_4 + \text{H} \rightleftharpoons \text{C}_2\text{H}_5$  reaction system. The H-abstraction is pressure-independent while the H-addition depends on pressure.

## References

1. W. C. Gardiner, *Gas-phase combustion chemistry*, Springer, New York, 2000.
2. D. L. Baulch, C. T. Bowman, C. J. Cobos, R. A. Cox, T. Just, J. A. Kerr, M. J. Pilling, D. Stocker, J. Troe, W. Tsang, R. W. Walker and J. Warnatz, *J. Phys. Chem. Ref. Data*, 2005, **34**, 757-1397.
3. J. A. Miller, M. J. Pilling and J. Troe, *Proc. Combust. Inst.*, 2005, **30**, 43-88.
4. V. D. Knyazev, A. Bencsura, S. I. Stoliarov and I. R. Slagle, *J. Phys. Chem.*, 1996, **100**, 11346-11354.
5. J. K. Shao, R. Choudhary, Y. Z. Peng, D. F. Davidson and R. K. Hanson, *J. Phys. Chem. A*, 2019, **123**, 15-20.
6. A. B. Callear and G. B. Smith, *Chem. Phys. Lett.*, 1984, **105**, 119-122.
7. T. Just, P. Roth and R. Damm, *Symp. Combust. Proc.*, 1977, **16**, 961-969.
8. N. S. Nametkin, L. V. Shevelkova and R. A. Kalinenko, *Dokl Akad Nauk SSSR*, 1975, **221**, 851-853.
9. Y. P. Yampolskii and N. S. Nametkin, *Kinet. Catal.*, 1976, **17**, 46-52.
10. G. B. Skinner, R. C. Sweet and S. K. Davis, *J. Phys. Chem.*, 1971, **75**, 1-&.
11. B. Ruscic, R. E. Pinzon, G. von Laszewski, D. Kodeboyina, A. Burcat, D. Leahy, D. Montoya and A. F. Wagner, *J. Phys. Conf. Ser.*, 2005, **16**, 561-570.
12. B. Ruscic, R. E. Pinzon, M. L. Morton, G. von Laszewski, S. J. Bittner, S. G. Nijsure, K. A. Amin, M. Minkoff and A. F. Wagner, *J. Phys. Chem. A*, 2004, **108**, 9979-9997.
13. B. Ruscic and D. H. Bross, Active Thermochemical Tables (ATcT) values based on ver. 1.122r of the Thermochemical Network (2021), available at ATcT.anl.gov.
14. T. L. Nguyen and J. F. Stanton, *J. Phys. Chem. A*, 2020, **124**, 2907-2918.
15. T. L. Nguyen and J. F. Stanton, *J. Phys. Chem. Lett.*, 2020, **11**, 3712-3717.
16. T. L. Nguyen and J. F. Stanton, *J. Phys. Chem. A*, 2018, **122**, 7757-7767.
17. T. L. Nguyen and J. F. Stanton, *J. Phys. Chem. A*, 2015, **119**, 7627-7636.
18. T. L. Nguyen, H. Lee, D. A. Matthews, M. C. McCarthy and J. F. Stanton, *J. Phys. Chem. A*, 2015, **119**, 5524-5533.
19. A. Tajti, P. G. Szalay, A. G. Csaszar, M. Kallay, J. Gauss, E. F. Valeev, B. A. Flowers, J. Vazquez and J. F. Stanton, *J. Chem. Phys.*, 2004, **121**, 11599-11613.
20. Y. J. Bomble, J. Vazquez, M. Kallay, C. Michauk, P. G. Szalay, A. G. Csaszar, J. Gauss and J. F. Stanton, *J. Chem. Phys.*, 2006, **125**, 064108.
21. M. E. Harding, J. Vazquez, B. Ruscic, A. K. Wilson, J. Gauss and J. F. Stanton, *J. Chem. Phys.*, 2008, **128**, 114111.
22. B. Ruscic and D. H. Bross, *Mol. Phys.*, 2021, **119**, e1969046.
23. J. H. Thorpe, J. L. Kilburn, D. Feller, P. B. Changala, D. H. Bross, B. Ruscic and J. F. Stanton, *J. Chem. Phys.*, 2021, **155**, 184109.
24. Y. G. Ren, L. Zhou, A. Mellouki, V. Daele, M. Idir, S. S. Brown, B. Ruscic, R. S. Paton, M. R. McGillen and A. R. Ravishankara, *Atmos. Chem. Phys.*, 2021, **21**, 13537-13551.
25. Y. C. Chang, B. Xiong, D. H. Bross, B. Ruscic and C. Y. Ng, *Phys. Chem. Chem. Phys.*, 2017, **19**, 9592-9605.
26. P. B. Changala, T. L. Nguyen, J. H. Baraban, G. B. Ellison, J. F. Stanton, D. H. Bross and B. Ruscic, *J. Phys. Chem. A*, 2017, **121**, 8799-8806.

27. D. Feller, D. H. Bross and B. Ruscic, *J. Phys. Chem. A*, 2017, **121**, 6187-6198.
28. D. Feller, D. H. Bross and B. Ruscic, *J. Phys. Chem. A*, 2019, **123**, 3481-3496.
29. B. K. Welch, R. Dawes, D. H. Bross and B. Ruscic, *J. Phys. Chem. A*, 2019, **123**, 5673-5682.
30. D. H. Bross, H. G. Yu, L. B. Harding and B. Ruscic, *J. Phys. Chem. A*, 2019, **123**, 4212-4231.
31. D. P. Zaleski, R. Sivaramakrishnan, H. R. Weller, N. A. Seifert, D. H. Bross, B. Ruscic, K. B. Moore, S. N. Elliott, A. V. Copan, L. B. Harding, S. J. Klippenstein, R. W. Field and K. Prozument, *J. Am. Chem. Soc.*, 2021, **143**, 3124-3142.
32. T. H. Dunning, *J. Chem. Phys.*, 1989, **90**, 1007-1023.
33. MRCC, a quantum chemical program suite written by M. Kállay, P. R. Nagy, D. Mester, Z. Rolik, G. Samu, J. Csontos, J. Csóka, P. B. Szabó, L. Gyevi-Nagy, B. Hégyel, I. Ladjánszki, L. Szegedy, B. Ladóczki, K. Petrov, M. Farkas, P. D. Mezei, and Á. Ganyecz See M. Kállay, P. R. Nagy, D. Mester, Z. Rolik, G. Samu, J. Csontos, J. Csóka, P. B. Szabó, L. Gyevi-Nagy, B. Hégyel, I. Ladjánszki, L. Szegedy, B. Ladóczki, K. Petrov, M. Farkas, P. D. Mezei, and Á. Ganyecz, *J. Chem. Phys.*, 2020, **152**, 074107, as well as: [www.mrcc.hu](http://www.mrcc.hu).
34. I. M. Mills, 1972, *Vibration-Rotation Structure in Asymmetric- and Symmetric-Top Molecules*. In *Molecular Spectroscopy: Modern Research*; Rao, K. N.; Mathews, C. W., Ed.; Academic Press: New York. **1972**, Vol. 1, pp. 115-140.
35. D. A. Matthews, L. Cheng, M. E. Harding, F. Lipparini, S. Stopkowicz, T. C. Jagau, P. G. Szalay, J. Gauss and J. F. Stanton, *J. Chem. Phys.*, 2020, **152**, 214108.
36. H. Eyring, *J. Chem. Phys.*, 1935, **3**, 107-115.
37. M. G. Evans and M. Polanyi, *Trans. Faraday Soc.*, 1935, **31**, 0875-0893.
38. T. Baer and W. L. Hase, *Unimolecular reaction dynamics : theory and experiments*, Oxford University Press, New York, 1996.
39. W. Forst, *Unimolecular reactions : a concise introduction*, Cambridge University Press, Cambridge, U.K. ; New York, 2003.
40. W. Forst, *Theory of unimolecular reactions*, Academic Press, New York, 1973.
41. W. H. Miller, *Faraday Discuss.*, 1977, **62**, 40-46.
42. W. H. Miller, R. Hernandez, N. C. Handy, D. Jayatilaka and A. Willetts, *Chem. Phys. Lett.*, 1990, **172**, 62-68.
43. R. Hernandez and W. H. Miller, *Chem. Phys. Lett.*, 1993, **214**, 129-136.
44. T. L. Nguyen, J. F. Stanton and J. R. Barker, *Chem. Phys. Lett.*, 2010, **499**, 9-15.
45. T. L. Nguyen, J. F. Stanton and J. R. Barker, *J. Phys. Chem. A*, 2011, **115**, 5118-5126.
46. W. H. Miller, *J. Am. Chem. Soc.*, 1979, **101**, 6810-6814.
47. J. R. Barker, T. L. Nguyen, J. F. Stanton, C. Aieta, M. Ceotto, F. Gabas, T. J. D. Kumar, C. G. L. Li, L. L. Lohr, A. Maranzana, N. F. Ortiz, J. M. Preses, J. M. Simmie, J. A. Sonk and P. J. Stimac, *MultiWell Program Suite*, University of Michigan, Ann Arbor, MI, 2017; see also: J. R. Barker, *Int. J. Chem. Kinet.* 2001, **33**, 232-245.
48. D. R. Glowacki, C. H. Liang, C. Morley, M. J. Pilling and S. H. Robertson, *J. Phys. Chem. A*, 2012, **116**, 9545-9560.
49. S. H. Robertson, D. R. Glowacki, C. Morley, C. H. Liang, R. J. Shannon, M. Blitz, P. Seakins, M. J. Pilling and J. N. Harvey, *MESMER: An Open-Source Master Equation Solver for Multi-Energy Well Reactions*, University of Leeds, Leeds, 2018.
50. S. J. Klippenstein, A. F. Wagner, S. H. Robertson, R. Dunbar and D. Wardlaw, *VARIFLEX*, Argonne National Laboratory, Lemont, IL, US, 1999.

51. Y. Georgievskii and S. J. Klippenstein, *MESS, Argonne National Laboratory, Lemont, IL, US*, 2016.
52. R. G. Gilbert, M. J. T. Jordan and S. C. Smith, *SSUMES : Steady-State Unimolecular Master-Equation Solver*, Sydney university, 1993.
53. V. Mokrushin, V. Bedanov, W. Tsang, M. R. Zachariah, V. D. Knyazev and W. S. McGivern, *ChemRate*, V. 1.5.10, April 14, 2011, National Institute of Standards and Technology, Gaithersburg, MD, 2011.
54. M. A. Hanning-Lee, N. J. B. Green, M. J. Pilling and S. H. Robertson, *J. Phys. Chem.*, 1993, **97**, 860-870.
55. J. A. Miller and S. J. Klippenstein, *Phys. Chem. Chem. Phys.*, 2004, **6**, 1192-1202.
56. S. C. Smith, M. J. McEwan and J. I. Brauman, *J. Phys. Chem. A*, 1997, **101**, 7311-7314.
57. S. J. Jeffery, K. E. Gates and S. C. Smith, *J. Phys. Chem.*, 1996, **100**, 7090-7096.
58. S. H. Robertson, M. J. Pilling, K. E. Gates and S. C. Smith, *J. Comput. Chem.*, 1997, **18**, 1004-1010.
59. J. A. Miller, S. J. Klippenstein and C. Raffy, *J. Phys. Chem.*, 2002, **106**, 4904-4913.
60. A. W. Jasper, K. M. Pelzer, J. A. Miller, E. Kamarchik, L. B. Harding and S. J. Klippenstein, *Science*, 2014, **346**, 1212-1215.
61. J. Troe, *J. Chem. Phys.*, 1977, **66**, 4745-4757.
62. R. C. Reid, J. M. Prausnitz and T. K. Sherwood, *The Properties of Gases and Liquids*, McGraw-Hill, New York, 1977.
63. P. D. Neufeld, R. A. Aziz and A. R. Janzen, *J. Chem. Phys.*, 1972, **57**, 1100-&.
64. J. M. Bowman, *J. Phys. Chem.*, 1991, **95**, 4960-4968.
65. N. Balakrishnan, *J. Chem. Phys.*, 2003, **119**, 195-199.
66. P. J. Robinson and K. A. Holbrook, *Unimolecular reactions*, Wiley-Interscience, London, New York, 1972.
67. K. A. Holbrook, M. J. Pilling, S. H. Robertson and P. J. Robinson, *Unimolecular reactions*, 2nd edn., Wiley, Chichester, New York, 1996.
68. N. J. B. Green, P. J. Marchant, M. J. Perona, M. J. Pilling and S. H. Robertson, *J. Chem. Phys.*, 1992, **96**, 5896-5907.
69. R. B. Lehoucq, D. C. Sorensen, and C. Yang, *ARPAC Users' Guide*, Society for Industrial and Applied Mathematics, Philadelphia, 1998.
70. E. Anderson, Z. Bai, C. Bischof, S. Blackford, J. Demmel, J. Dongarra, J. Du Croz, A. Greenbaum, S. Hammarling, A. McKenney and D. Sorensen, *LAPAC Users' Guide*, Society for Industrial and Applied Mathematics, Philadelphia, 1999.
71. E. Anderson and J. J. Dongarra, *Performance of LAPACK : a portable library of numerical linear algebra routines*, University of Tennessee, Knoxville, Tenn., 1992.
72. J. R. Barker, J. F. Stanton and T. L. Nguyen, *Int. J. Chem. Kinet.*, 2020, **52**, 1022-1045.
73. T. L. Nguyen, L. McCaslin, M. C. McCarthy and J. F. Stanton, *J. Chem. Phys.*, 2016, **145**, 131102.
74. T. L. Nguyen, J. H. Thorpe, D. H. Bross, B. Ruscic and J. F. Stanton, *J. Phys. Chem. Lett.*, 2018, **9**, 2532-2538.
75. T. L. Nguyen, B. Ruscic and J. F. Stanton, *J. Chem. Phys.*, 2019, **150**.
76. F. D. Rossini and J. W. Knowlton, *J. Res. Nat. Bur. Stand.*, 1937, **19**, 249-262.

77. F. D. Rossini, K. S. Pitzer, W. J. Taylor, J. P. Ebert, J. E. Kilpatrick, C. W. Beckett, M. G. Williams and H. G. Werner, *Selected Values of Properties of Hydrocarbons*, Natl. Bur. Stand. Circular 461, U.S. Gov. Printing Office: Washington, DC 1947.
78. F. D. Rossini, D. D. Wagman, W. E. Evans, S. Levine and I. Jaffe, *Selected Values of Chemical Thermodynamic Properties*, Natl. Bur. Stand. Circular 500, U.S. Gov. Printing Office: Washington, DC 1952.
79. D. D. Wagman, W. H. Evans, I. Halow, V. B. Parker, S. M. Bailey and R. H. Schumm, *Selected Values of Chemical Thermodynamic Properties. Tables for the First Thirty-Four Elements in the Standard Order of Arrangement*, NBS Technical Note 270-3, U.S. Gov. Printing Office: Washington, DC 1968.
80. D. D. Wagman, W. H. Evans, V. B. Parker, R. H. Schumm, I. Halow, S. M. Bailey, K. L. Churney and R. L. Nuttall, *The NBS Tables of Chemical Thermodynamic Properties*, *J. Phys. Chem. Ref. Data*, 1982, **11**, Suppl. 2.
81. J. D. Cox and G. Pilcher, *Thermochemistry of Organic and Organometallic Compounds*, Academic: London 1970.
82. D. R. Stull and H. Prophet, Proj. Dirs., *JANAF Thermochemical Tables*, 2nd ed., NSRDS-NBS 37, Natl. Bur. Std., U.S. Gov. Printing Office, Washington, DC 1971.
83. M. W. Chase, C. A. Davies, J. R. Downey, D. J. Frurip, R. A. McDonald and A. N. Syverud, *JANAF Thermochemical Tables*, 3rd ed., *J. Phys. Chem. Ref. Data.*, 1985, **14**, Suppl. 1.
84. M. W. Chase Jr., Ed., *NIST-JANAF Thermochemical Tables*, 4th ed., *J. Phys. Chem. Ref. Data*, 1998, Monogr. 9.
85. J. Chao and B. J. Zwolinski, *J. Phys. Chem. Ref. Data* 1975, **4**, 251-261.
86. *Selected Values of Properties of Hydrocarbons and Related Compounds*, TRC Tables, Thermodynamics Research Center, Texas A&M University, College Station, TX 1985
87. J. B. Pedley, R. D. Naylor, and S. P. Kirby, *Thermochemical Data of Organic Compounds*, 2nd ed., Chapman and Hall, London 1986.
88. V. P. Glushko, L. V. Gurvich, G. A. Bergman, I. V. Veic, V. A. Medvedev, G. A. Khachkuruzov, and V. S. Iungman, *Termodinamicheskie svoistva individual'nykh veshchestv*, 3rd. Ed, Vol. 2, Parts 1 and 2, Nauka, Moscow 1979.
89. L. V. Gurvich, I. V. Veyts, and C. B. Alcock, eds., *Thermodynamic Properties of Individual Substances*, Vol. 2, Parts One and Two, 4th ed., Hemisphere, New York 1990.
90. J. A. Manion, *J. Phys. Chem. Ref. Data*, 2002, **31**, 123-172.
91. B. Ruscic, *J. Phys. Chem. A*, 2015, **119**, 7810-7837.
92. B. Ruscic, D. Feller and K. A. Peterson, *Theor. Chem. Acc.*, 2014, **133**, 1415.
93. J. Berkowitz, C. A. Mayhew and B. Ruscic, *J. Chem. Phys.*, 1988, **88**, 7396-7404.
94. K. M. Ervin, S. Gronert, S. E. Barlow, M. K. Gilles, A. G. Harrison, V. M. Bierbaum, C. H. Depuy, W. C. Lineberger and G. B. Ellison, *J. Am. Chem. Soc.*, 1990, **112**, 5750-5759.
95. W. Tsang, *Heats of Formation of Organic Free Radicals by Kinetic Methods*, in: *Energetics of Organic Free Radicals*, J.A. Martinho Simoes, A. Greenberg, and J. F. Liebman, Eds., Blackie Academic: London 1996, pp. 22-58.
96. A. Karton, E. Rabinovich, J. M. L. Martin and B. Ruscic, *J. Chem. Phys.*, 2006, **125**.
97. A. Karton, A. Tarnopolsky, J. F. Lamere, G. C. Schatz and J. M. L. Martin, *J. Phys. Chem. A*, 2008, **112**, 12868-12886.
98. A. Karton, S. Daon and J. M. L. Martin, *Chem. Phys. Lett.*, 2011, **510**, 165-178.

99. D. P. Tabor, M. E. Harding, T. Ichino and J. F. Stanton, *J. Phys. Chem. A*, 2012, **116**, 7668-7676.
100. S. J. Klippenstein, L. B. Harding and B. Ruscic, *J. Phys. Chem. A*, 2017, **121**, 6580-6602.
101. J. Aguilera-Iparraguirre, A. D. Boese, W. Klopper and B. Ruscic, *Chem. Phys.*, 2008, **346**, 56-68.
102. E. W. Kaiser and T. J. Wallington, *J. Phys. Chem.*, 1996, **100**, 4111-4119.
103. B. Ruscic, J. Berkowitz, L. A. Curtiss and J. A. Pople, *J. Chem. Phys.*, 1989, **91**, 114-121.
104. P. W. Seakins, M. J. Pilling, J. T. Niiranen, D. Gutman and L. N. Krasnoperov, *J. Phys. Chem.*, 1992, **96**, 9847-9855.
105. A. Bodi, J. P. Kercher, C. Bond, P. Meteesatien, B. Sztaray and T. Baer, *J. Phys. Chem. A*, 2006, **110**, 13425-13433.
106. N. Leplat, A. Wokaun and M. J. Rossi, *J. Phys. Chem. A*, 2013, **117**, 11383-11402.
107. M. A. Blitz, M. J. Pilling, S. H. Robertson, P. W. Seakins and T. H. Speak, *J. Phys. Chem. A*, 2021, **125**, 9548-9565.
108. M. Brouard, P. D. Lightfoot and M. J. Pilling, *J. Phys. Chem.*, 1986, **90**, 445-450.
109. O. Dobis and S. W. Benson, *J. Phys. Chem. A*, 1997, **101**, 6030-6042.
110. G. C. Fettes, J. H. Knox and A. F. Trotmandickenson, *J. Chem. Soc.*, 1960, 4177-4185.
111. T. J. Sears, P. M. Johnson and J. BeeBe-Wang, *J. Chem. Phys.*, 1999, **111**, 9213-9221.
112. B. Ruscic and D. H. Bross, *Computer Aided Chem. Eng.*, 2019, **45**, 3-114.
113. J. Agarwal, J. M. Turney and H. F. Schaefer, *J. Phys. Chem. Lett.*, 2011, **2**, 2587-2592.
114. Y. L. Fu, X. X. Lu, Y. C. Han, B. N. Fu, D. H. Zhang and J. M. Bowman, *Chem. Sci.*, 2020, **11**, 2148-2154.
115. J. V. Michael, D. T. Osborne and G. N. Suess, *J. Chem. Phys.*, 1973, **58**, 2800-2806.
116. J. V. Michael, M. C. Su, J. W. Sutherland, L. B. Harding and A. F. Wagner, *Proc. Combust. Inst.*, 2005, **30**, 965-973.
117. P. D. Lightfoot and M. J. Pilling, *J. Phys. Chem.*, 1987, **91**, 3373-3379.
118. Y. Feng, J. T. Niiranen, A. Bencsura, V. D. Knyazev, D. Gutman and W. Tsang, *J. Phys. Chem.*, 1993, **97**, 871-880.
119. S. E. Stein and A. Fahr, *J. Phys. Chem.*, 1985, **89**, 3714-3725.
120. K. O. Johansson, M. P. Head-Gordon, P. E. Schrader, K. R. Wilson and H. A. Michelsen, *Science*, 2018, **361**, 997-1000.
121. J. A. Miller and S. J. Klippenstein, *J. Phys. Chem. A*, 2003, **107**, 7783-7799.
122. J. A. Miller, S. J. Klippenstein, Y. Georgievskii, L. B. Harding, W. D. Allen and A. C. Simmonett, *J. Phys. Chem. A*, 2010, **114**, 4881-4890.
123. V. S. Krasnoukhov, D. P. Porfiriev, I. P. Zavershinskiy, V. N. Azyazov and A. M. Mebel, *J. Phys. Chem. A*, 2017, **121**, 9191-9200.
124. B. J. Gaynor, R. G. Gilbert, K. D. King and P. J. Harman, *Aust. J. Chem.*, 1981, **34**, 449-452.
125. C. F. Melius, M. E. Colvin, N. M. Marinov, W. J. Pitz and S. M. Senkan, *Proc. Combust. Inst.*, 1996, **26**, 685-692.
126. A. W. Jasper and N. Hansen, *Proc. Combust. Inst.*, 2013, **34**, 279-287.
127. S. Sharma and W. H. Green, *J. Phys. Chem. A*, 2009, **113**, 8871-8882.
128. B. K. Carpenter, G. B. Ellison, M. R. Nimlos, and A. M. Scheer, *J. Phys. Chem. A*, 2022, <https://doi.org/10.1021/acs.jpca.2c00038>.
129. J. A. Miller and S. J. Klippenstein, *J. Phys. Chem. A*, 2001, **105**, 7254-7266.

130. V. V. Kislov, T. L. Nguyen, A. M. Mebel, S. H. Lin and S. C. Smith, *J. Chem. Phys.*, 2004, **120**, 7008-7017.
131. L. B. Harding, *J. Am. Chem. Soc.*, 1981, **103**, 7469-7475.
132. A. Matsugi, *J. Phys. Chem. Lett.*, 2013, **4**, 4237-4240.
133. H. Hippler, J. Troe and H. J. Wendelken, *J. Chem. Phys.*, 1983, **78**, 6718-6724.